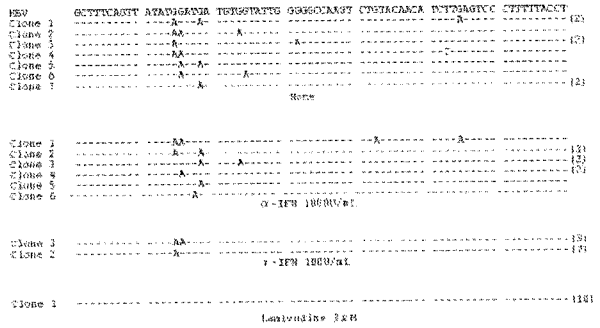

Fig. 6. Nucleotide sequence substitutions around YMDD motif of reverse transcriptase detected by PCR with PNA clamping after treating a HepG2 cell line (cell line 2 in Table 3). The nucleotide sequence of the transfected clone was used as a reference sequence (**top line**). Cells were treated with interferons and lamivudine as shown in Figs. 5 and 7, respectively.

noticeable increase in HepG2 cells by our detection method (C. Noguchi and K. Chayama, unpublished data). However, the method employed to detect hypermutation is not quantitative. Moreover, no antibody to detect APOBEC3G is available. Measurement of activity of this enzyme might be necessary to address this issue.

Because the patterns of hypermutations found in patients as well as cell lines are in agreement with strong dinucleotide preferences of a retroviral genome[31-35] edited by APOBEC3G,[7-9] we assume that hypermutations might also be induced by a similar enzyme. As pointed out by Turelli et al.,[20-29] another deaminase including APOBEC3F might be responsible for the generation of hypermutation. We actually detected the expression of deaminases in HepG2 cell lines. The expression levels of these deaminases are very low because they were detected by only two-stage PCR with one exception (only APOBEC3F was detected by a single-stage PCR).

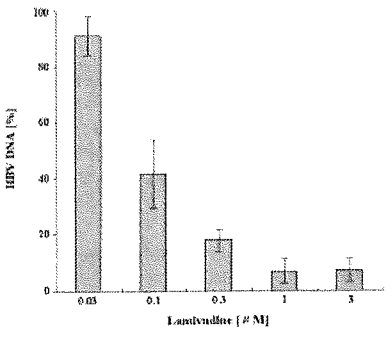


Fig. 7. Effects of lamivudine on production of HBV DNA by cell line 1. After 5 days of lamivudine treatment, the HBV DNA in core particles was immunoprecipitated and quantitated by real-time PCR. Data are mean ± SD of 4 independent experiments.

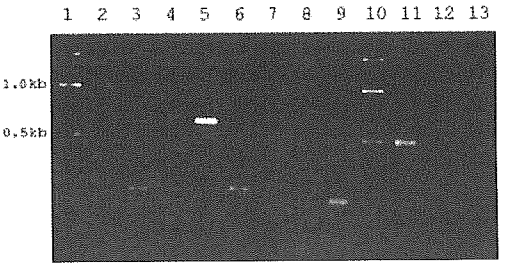


Fig. 8. Agarose gel electrophoresis of mRNAs of known deaminases amplified by reverse transcription-polymerase chain reaction. Lane 1: molecular weight size marker; lane 2: APOBEC1; lane 3: APOBEC2; lane 4: APOBEC3A; lane 5: APOBEC3B; lane 6: APOBEC3C; lane 7: APOBEC3D; lane 8: APOBEC3F; lane 9: APOBEC3G; lane 10: molecular weight size marker. Only mRNA of APOBEC3F was detected by one-stage PCR. To confirm the predictability of the assay, 3 negative mRNAs in Hep3G (APOBEC1, 3A and 3D) were amplified by using mRNAs from tissues known to express it. Lanes 11 and 12: APOBEC1 and APOBEC3A from the ileum; lane 13: APOBEC3D from the duodenum. All detected cDNAs were cloned, and nucleotide sequences were confirmed.

However, other possibilities should not be ignored. For example, some viral proteins might prevent such editing activity of deaminase by associating with this enzyme, as virion infectivity factor does in HIV-1–infected cells. Possibly the edited HBV genomes are degraded in liver cells rapidly by removal of the U residues by uracil DNA glycocylase followed by cellular nucleases.[36]

We found hypermutated genomes only in patients positive for eAb. The G to A nucleotide substitution of codon 28 of pre-core protein, which induces premature stop of this protein and basal core promoter mutations (A1762T/G1764A), might be related to the clearance of eAg.[28] Further studies should be conducted to investigate the relationship between G to A substitutions in these regions by deaminase(s), production of eAg, and replication efficacy of the virus.

A recent study showed that the amount of HBV DNA reduction occurs noncytopathologically through the action of cytokines, especially interferon alpha/beta and gamma.[37,38] We thus examined whether interferon can alter the occurrence of hypermutation. However, the results showed no increase in the number of hypermutation in HepG2–derived cell lines treated by interferon alpha and gamma (Fig. 6). Thus, the antiviral action of the mechanism responsible for G to A substitution in liver cells is likely to be independent of the action of interferon.

In conclusion, numerous innate intracellular defense systems exist, and the precise pathways of such systems are not fully understood. The role of editing of the HBV genome in such defense systems should be further investigated to understand the natural antiviral mechanisms and to develop an antiviral strategy against HBV.

*Acknowledgment:* A part of this work was carried out at the Research Center for Molecular Medicine, Faculty of Medicine, and Liver Research Project Center, Hiroshima University, Hiroshima, Japan. The authors thank thank Eiko Okutani, Yukiji Tonouchi and Kiyomi Toyota for their excellent technical assistance.

## References

1. Wright TL, Lau JY. Clinical aspects of hepatitis B virus infection. Lancet 1993;342:1340-1344.
2. Bruix J, Llovet JM. Hepatitis B virus and hepatocellular carcinoma. J Hepatol 2003;39(Suppl 1):S59-S63.
3. Raimondo G, Pollicino T, Squadrito G. Clinical virology of hepatitis B virus infection. J Hepatol. 2003;39(Suppl 1):S26-S30.
4. Ganem D, Prince AM. Hepatitis B virus infection: Natural history and clinical consequences. N Engl J Med 2004;350:1118-1129.
5. Ganem D, Schneider R. Hepadnaviridae: The Virus and Their Replication. Volume 3. 4th ed. Philadelphia: Lippincott-Raven Publishers, 2001.
6. Skalka AM, Goff SP. Reverse Transcriptase. Cold Spring Harbor, NY: Cold Spring Harbor Laboratory Press, 1993.
7. Mangeat B, Turelli P, Caron G, Friedli M, Perrin L, Trono D. Broad antiretroviral defense by human APOBEC3G through lethal editing of nascent reverse transcripts. Nature 2003;424:99-103.
8. Zhang HYB, Pomerantz RJ, Zhang C, Arunachalam SC, Gao L. The cytidine deaminase CEM15 induces hypermutation in newly synthesized HIV-1 DNA. Nature 2003;424:94-98.
9. Lecossier D, Bouchonnet F, Clavel F, Hance AJ. Hypermutation of HIV-1 DNA in the absence of the Vif protein. Science 2003;300:1112.
10. Harris RS, Bishop KN, Shechy AM, Craig HM, Petersen-Mahrt SK, Watt IN, et al. DNA deamination mediates innate immunity to retroviral infection. Cell 2003;113:803-809.
11. Mariani R, Chen D, Schrofelbauer B, Navarro F, Konig R, Bollman B, et al. Species-specific exclusion of APOBEC3G from HIV-1 virions by Vif. Cell 2003;114:21-31.
12. Kobayashi M, Takaori-Kondo A, Shindo K, Abudu A, Fukunaga K, Uchiyama T. APOBEC3G targets specific virus species. J Virol 2004;78:8238-8244.
13. Shindo K, Takaori-Kondo A, Kobayashi M, Abudu A, Fukunaga K, Uchiyama T. The enzymatic activity of CEM15/Apobec-3G Is essential for the regulation of the infectivity of HIV-1 virion but not a sole determinant of its antiviral activity. J Biol Chem 2003;278:44412-44416.
14. Li J, Porash MJ, Volsky DJ. Functional domains of APOBEC3G required for antiviral activity. J Cell Biochem 2004;92:560-572.
15. Liu B, Yu X, Luo K, Yu Y, Yu XF. Influence of primate lentiviral Vif and proteasome inhibitors on human immunodeficiency virus type 1 virion packaging of APOBEC3G. J Virol 2004;78:2072-2081.
16. Mehle A, Strack B, Ancuta P, Zhang C, McPike M, Gabuzda D. Vif overcomes the innate antiviral activity of APOBEC3G by promoting its degradation in the ubiquitin-proteasome pathway. J Biol Chem 2004;279:7792-7798.
17. Marin M, Rose KM, Kozak SL, Kabat D. HIV-1 Vif protein binds the editing enzyme APOBEC3G and induces its degradation. Nat Med 2003;9:1398-1403.
18. Stopak K, de Noronha C, Yonemoto W, Greene WC. HIV-1 Vif blocks the antiviral activity of APOBEC3G by impairing both its translation and intracellular stability. Mol Cell 2003;12:591-601.
19. Gunther S, Sommer G, Plikat U, Imaska A, Wain-Hobson S, Will H, et al. Naturally occurring hepatitis B virus genomes bearing the hallmarks of retroviral G→A hypermutation. Virology 1997;235:104-108.
20. Turelli P, Mangeat B, Jost S, Vianin S, Trono D. Inhibition of hepatitis B virus replication by APOBEC3G. Science 2004;303:1829.
21. Ohishi W, Shirakawa H, Kawakami Y, Kimura S, Kamiyasu M, Tazuma S, et al. Identification of rare polymerase variants of hepatitis B virus using a two-stage PCR with peptide nucleic acid clamping. J Med Virol 2004;72:558-565.
22. Rose PP, Korber BT. Detecting hypermutations in viral sequences with an emphasis of G to A hypermutation. Biofinformatics 2000;16:400-401.
23. Egholm M, Buchardt O, Christensen L, Behrens C, Freier SM, Driver DA, et al. PNA hybridizes to complementary oligonucleotides obeying the Watson-Crick hydrogen-bonding rules. Nature 1993;365:566-568.
24. Cabrerizo M, Bartolom J, Caramelo C, Barril G, Carreno V. Molecular analysis of hepatitis B virus DNA in serum and peripheral blood mononuclear cells from hepatitis B surface antigen-negative cases. HEPATOLOGY 2000;32:116-123.
25. Cabrerizo M, Baetolome J, Carreno V. In vitro infection of human peripheral blood mononuclear cells by a defective hepatitis B virus with a deletion in the PreS1 region of the viral genome. J Viral Hepatol 2002;9:265-271.
26. Zoulim F, Vitvitski L, Bouffard P, Pichoud C, Rougier P, Lamelin JP, et al. Detection of pre-S1 proteins in peripheral blood mononuclear cells from patients with HBV infection. J Hepatol 1991;12:150-156.
27. Murakami Y, Minami M, Daimon Y, Okanoue T. Hepatitis B virus DNA in liver, serum, and peripheral blood mononuclear cells after the clearance of serum hepatitis B virus surface antigen. J Med Virol 2004;72:203-214.
28. Milich D, Liang TJ. Exploring the biological basis of hepatitis B e antigen in hepatitis B virus infection. HEPATOLOGY 2003;38:1075-1086.
29. Turelli P, Jost S, Mangeat B, Trono D. Response to comment of "Inhibition of hepatitis B virus replication by APOBEC3G". Science 2004;305:1403b.
30. Rosler C, Kock J, Malim MH, Blum HE, Weizsacker F. Comment on "Inhibition of hepatitis B virus replication by APOBEC3G". Science 2004;305:1403a.
31. Koulinska I, Chaplin B, Mwakagile D, Essex M, Renjifo B. Hypermutation of HIV type 1 genomes isolated from infants soon after vertical infection. AIDS Res Hum Retrov 2003;19:1115-1123.
32. Vartanian J, Meterhans A, Sala M, Wain-Hobson S. Selection, recombination, and G→A hypermutation of human immunodeficiency virus type 1 genomes. J Virol 1991;65:1779-1788.
33. Janini M, Rogers M, Birx DR, McCutchan FE. Human Immunodeficiency virus type 1 DNA sequences genetically damaged by hypermutation are often abundant in patient peripheral blood mononuclear cells and may be generated during near-simultaneous infection and activation of CD4+ T cells. J Virol 2001;75:7973-7986.
34. Borman A, Quillent C, Charneau P, Kean KM, Clavel F. A highly defective HIV-1 group O provirus: evidence for the role of local sequence determinants in G→A hypermutation during negative-Strand viral DNA synthesis. Virology 1995;208:601-609.
35. Overbaugh J, Jackson S, Papenhausen M, Rudensey LM. Lentiviral genomes with G-to-A hypermutation may result from Taq polymerase errors during polymerase Chain reaction. AIDS Res Hum Retroviruses 1996;17:1605-1613.
36. Lindahl T, Wood RD. Quality control by DNA repair. Science 1999;286:1897-1905.
37. Guidotti LG, Ando K, Hobbs MV, Ishikawa T, Runkel L, Schreiber RD, et al. Cytotoxic T lymphocytes inhibit hepatitis B virus gene expression by a noncytolytic mechanism in transgenic mice. Proc Natl Acad Sci U S A 1994;91:3764-3768.
38. Guidotti LG, Ishikawa T, Hobbs MV, Matzke B, Schreiber R, Chisari FV. Intracellular inactivation of the hepatitis B virus by cytotoxic T lymphocytes. Immunity 1996;4:25-36.

*Digestive Diseases and Sciences, Vol. 50, No. 7 (July 2005), pp. 1361–1371 (© 2005)*
DOI: 10.1007/s10620-005-2788-1

# Hepatitis C Virus Core Protein Modulates Fatty Acid Metabolism and Thereby Causes Lipid Accumulation in the Liver

ATSUSHI YAMAGUCHI, MD,* SUSUMU TAZUMA, MD, PhD,† TOMOJI NISHIOKA, MD, PhD,* WAKA OHISHI, MD, PhD,* HIDEYUKI HYOGO, MD, PhD,† SHUICHI NOMURA, MD, PhD,† and KAZUAKI CHAYAMA, MD, PhD*

We studied the roles of hepatitis C virus (HCV) core protein in hepatic steatosis and changes in hepatic lipid metabolism. HCV core protein expression plasmid was transfected in HepG2 . Triacylglyceride (TG) and mRNA level associated with lipid metabolism were measured. Male C57BL/6 mice were infected with HCV core recombinant adenovirus and used for lipids and mRNA studies. In HCV core protein-expressing cells, peroxisome proliferator-activated receptor (PPAR)$\alpha$, multidrug resistance protein (MDR) 3, and microsomal triglyceride transfer protein (MTP) were down-regulated 48 hr after transfection. In HCV core protein-expressing mice, hepatic TG content and hepatic thiobarbituric acid-reactive substances increased. PPAR$\alpha$, MDR2, acyl-CoA oxidase (AOX), and carnitine palmitoyl transferase-1 (CPT-1) were down-regulated. HCV core protein down-regulated lipid metabolism-associated gene expression, Mdr2, CPT, and AOX, accompanied by down-regulation of PPAR$\alpha$. There findings may contribute to the understanding of HCV-related steatosis, induction of reactive oxygen species, and carcinogenesis.

**KEY WORDS:** HCV core protein; steatosis; nuclear receptor; ABC transporter.

Chronic hepatitis C virus (HCV) infection results in necroinflammatory liver disease that is characterized by the insidious progression of hepatic fibrosis and the loss of functioning hepatocytes (1–3). Little is known about the molecular mechanisms underlying liver injury due to infection with this virus, but a cell-mediated immune response associated with prominent lymphocytic infiltration of hepatic tissues is thought to play a major role (4, 5). In addition, various observations have suggested that nonimmune mechanisms may also play an important role. These findings include the frequent presence of hepatic steatosis in patients with chronic hepatitis C, an abnormality that is not often observed in other inflammatory conditions such as autoimmune hepatitis and chronic hepatitis B (6–9). Also, a considerable number of *in vitro* studies have suggested that expression of various HCV proteins may lead to alterations of lipid metabolism and transport, cell cycle dysregulation, increased or decreased susceptibility to apoptosis, and cellular transformation (10–17). In particular, HCV core protein has been suggested to contribute to hepatic steatosis (18–20), induction of reactive oxygen species (ROS) (19–21), and hepatic carcinogenesis (22).

Regarding HCV core protein-induced steatosis, the following findings have been reported: (a) HCV core protein interacts with apoA2, a major component of high-density lipoprotein (10, 23), (b) HCV core protein interferes with the assembly of very low-density lipoprotein (VLDL) by reducing the level of microsomal triglyceride transfer

Manuscript received October 7, 2004; accepted December 2, 2004.
From the Departments of *Medicine and Molecular Science and †General Medicine and Clinical Pharmacotherapy, Graduate School of Biomedical Sciences, Hiroshima University, Hiroshima, Japan.
Address for reprint requests: Susumu Tazuma MD, PhD, Department of General Medicine and Clinical Pharmacotherapy, Graduate School of Biomedical Sciences, Hiroshima University, 1-2-3 Kasumi, Minami-ku, Hiroshima, 734-8551, Japan; stazuma@hiroshima-u.ac.jp.

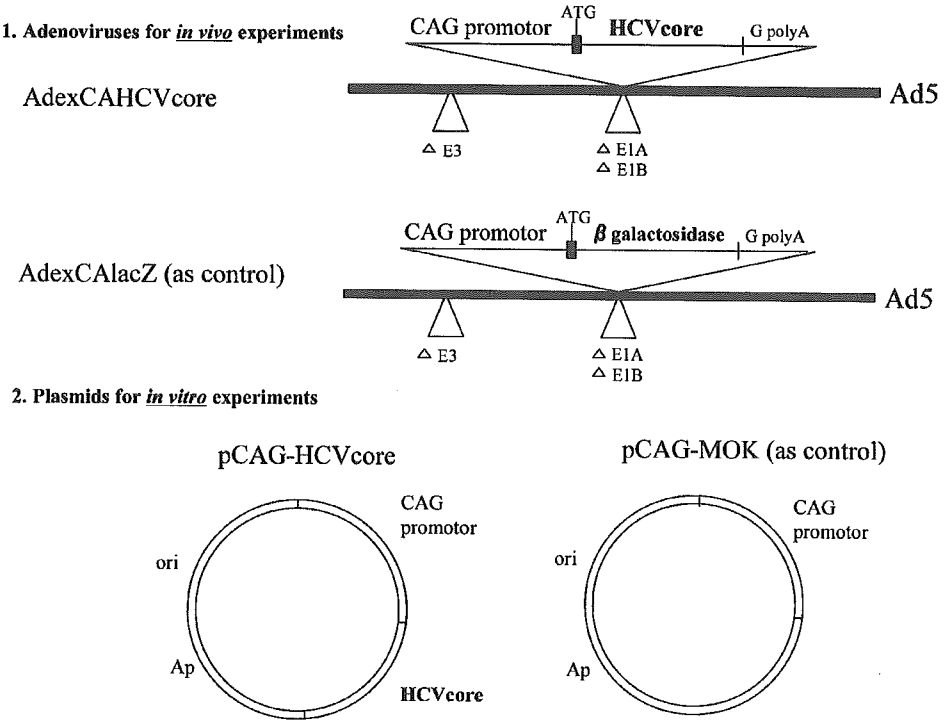


**Fig 1.** Constructs of recombinant adenoviruses and plasmids employed in this study. See Materials and Methods. ATG, start codon; G poly(A), rabbit $\beta$-globin poly(A); CAG promoter; cytomegalovirus enhancer, chicken $\beta$-actin promoter, and rabbit $\beta$-globin poly(A); Ad5, adenovirus type 5 genome lacking E1A, E1B, and E3.

protein (24), and (c) HCV core protein causes steatosis due to mitochondrial toxicity and production of ROS (19, 20). However, the details of the interaction between HCV and lipid metabolism remain unclear. Hepatocytes represent the crossroads of various metabolic pathways, so HCV may interfere with lipid metabolism via one or several pathways. To investigate the role of HCV core protein in steatosis and the accompanying changes in hepatic lipid metabolism, we focused on fatty acid metabolism-associated proteins, including those involved in fatty acid oxidation and lipid transport into blood and bile, as well as nuclear receptors.

## MATERIALS AND METHODS

**Plasmid and Recombinant Adenovirus.** The complementary DNA clone of the full-length HCV core protein (amino acids [aa] 1–191) was derived from the serum of a patient with HCV 1b by reverse transcription and nested polymerase chain reaction. First-strand primers were 5′-CTGCTAGCCGAGTAGTGTTG-3′ and 5′-CATTGAGGACCACCAGGTTCT-3′, while second-strand primers were 5′-CGGGAATTCTCGTAGACCGTGCACCATG AGC-3′ and 5′-GTTGGGATCCTCCTAAGCGGAAGCTGG GAT-3′. The gene was inserted into pBluescript (Stratagene, La Jolla, CA, USA) and cloned. Then it was made to correspond with HCV 132996 (GenBank) using a QuikChange Site-Directed Mutagenesis kit (Stratagene). The HCV core protein expression plasmid (pCAG-HCVcore), a control plasmid (MOK), and a $\beta$-galactosidase expression plasmid (pCAG-LacZ) were prepared using an adenovirus expression vector kit (Takara Biotechnology, Tokyo) (25, 26). The HCV core gene was inserted into the *Swa*I site in cosmid vector pAxCAwt, which is a 44.741-kilobase cosmid containing a 31-kilobase adenovirus type 5 genome lacking the E1A, E1B, and E3 genes, but including the cytomegalovirus enhancer, chicken $\beta$-actin promoter, and rabbit $\beta$-globin poly(A) signal (pAxCAiHCVcore). The cosmid vector pAxCAiLacZ, with the $\beta$-galactosidase gene inserted into pAxCAwt, was included in the adenovirus expression vector kit. These three vectors (pAxCAwt, pAxCAiHCVcore, and pAxCAiLacZ) were digested at the *Sal*I site and ligated, yielding the pCAG-MOK, pCAG-HCVcore, and pCAG-LacZ expression plasmids for cell transfection experiments. The cosmid pAxCAiHCVcore or pAxCAiLacZ was cotransfected into 293 cells with adenovirus DNA by calcium phosphate precipitation. Incorporation of the expression cassette was confirmed by digestion with *Cla*I. Recombinant adenovirus (AdexCAHCVcore or AdexCAlacZ) was propagated in 293 cells and the viral titer was determined as the 50% tissue culture infectious dose using 293 cells. These viruses were used for animal experiments (Figure 1).

**Cell Culture.** HepG2 cells were seeded into 56-cm$^2$ tissue culture dishes in Dulbecco's modified Eagle's medium (DMEM)

(Gibco, Grand Island, NY, USA) supplemented with 10% fetal bovine serum (FBS) (Sigma, St. Louis, MO, USA) and an antibiotic/antimycotic mixture (100 U/ml each) (Gibco) and were cultured in a humidified incubator (5% $CO_2$) at 37°C. The medium was replaced with fresh medium every 3–4 days. Prior to each experiment, the cells were seeded into 6- or 12-well plates and allowed to attach for at least 24 hr (6-well for triglyceride [TG] assay and 12-well for RNA extraction).

**Transfection.** Using SuperFect Transfection Reagent (Qiagen, Tokyo), cells were transfected with 4 or 3 $\mu$g of pCAG-HCVcore or pCAG-MOK (4 $\mu$g for 6-well plates and 3 $\mu$g for 12-well plates) and were cultured in DMEM with 10% FBS. After 24 or 48 hr, the cells were harvested for analysis. The efficiency of transfection was investigated using pCAG-LacZ. Cells were washed with phosphate-buffered saline (PBS) and fixed with 2% formaldehyde and 0.2% glutaraldehyde in PBS. Then the cells were stained with X-gal using a $\beta$-Gal Staining Set (Roche, Tokyo).

**Animals.** Adult male C57BL/6 mice (Charles River Laboratories, Yokohama, Japan), which were over 8 weeks old and weighed 21–24 g, were used in this study. All animals were housed in an environmentally controlled facility with a 12-hr lighting time (lights on from 0700 until 1900 hr). They were given free access to standard chow and water. Experiments (intravenous injection and sacrifice) were performed from 0900 to 21 hr. The animals received humane care according to the institutional guidelines for handling experimental animals.

**HCV Core Protein Expression in Mice.** The animals received an intravenous injection of $1 \times 10^9$ pfu (plaque-forming units) of AdexCAHCVcore or AdexCAlacZ and were sacrificed 3 days later. Mice were anesthetized with pentobarbital (100 mg/kg intraperitoneally). Blood was collected by cardiac puncture with a heparinized syringe, after which the liver was rapidly removed, weighed, and perfused with ice-cold PBS (pH 7.4). Part of the liver was fixed in 10% neutral buffered formalin and embedded in paraffin for histologic analysis. Another part was stored in RNA later reagent (Qiagen, Tokyo) at 4°C for extraction of RNA, and the remaining liver tissue was snap-frozen in liquid nitrogen and stored at −80°C until required. Plasma was immediately separated by centrifugation (10,000 rpm at 4°C) and stored at −20°C.

**Liver Histology and Serum ALT Level.** Sections of liver tissue (4 $\mu$m thick) were stained with hematoxylin and eosin for analysis. The serum alanine aminotransferase (ALT) level was measured using an automated technique by SRL Co. (Hiroshima, Japan).

**HCV Core Protein Expression in Cells.** Proteins were extracted from cells using PRO-PREP protein extraction solution (containing 1.0 mM PMSF, 1.0 mM EDTA, 1 $\mu$M pepstatin, 1 $\mu$M leupeptin, and 1 $\mu$M aprotinin) (Intron Biotechnology, Kyungki-Do, Korea). HCV core antigen levels were measured in cells using an HCV core antigen enzyme-linked immunosorbent assay (ELISA) (Ortho-Clinical Diagnostics K.K., Tokyo).

**HCV Core Protein Expression in Mice.** We confirmed HCV core protein expression in liver tissue by Western blot analysis. Proteins were extracted using PRO-PREP protein extraction solution. Then 50 $\mu$g of protein was separated by sodium dodecyl sulfate–polyacrylamide gel electrophoresis and transferred to a nitrocellulose membrane (Millipore, Bedford, MA, USA) using a tank blotting system according to the manufacturer's instructions (Bio-Rad Laboratories). After transfer, the membrane was blocked for 2 hr at room temperature with 5% powdered skim milk dissolved in Tris-buffered saline containing 0.05% between 20 and then incubated overnight at 4°C with a monoclonal mouse antibody to HCV core protein (kindly provided by Ortho-Clinical Diagnostics K.K.). Immune complexes were detected using alkaline phosphatase-conjugated anti-mouse IgG (Cosmo Bio, Tokyo) according to the manufacturer's instructions (Bio-Rad Laboratories). Detection of HCV core protein was performed by comparison with the following standards: myosin (200 kDa), $\beta$-galactosidase (116 kDa), bovine serum albumin (66 kDa), carbonic anhydrase (31 kDa), soybean trypsin inhibitor (21.5 kDa), lysozyme (14.4 kDa), and aprotinin (6.5 kDa).

**Measurement of Triglyceride Content.** After the medium was removed, the cells were washed three times with PBS and resuspended in 200 $\mu$l of PBS. Then lipids were extracted from 100 $\mu$l of PBS by the method of Bligh and Dyer (27) and resuspended in 100 $\mu$L of 10% Triton X. The cellular content of TG was measured using enzyme reagents and standards from Wako (Osaka, Japan). The remainder of the PBS suspension was used for the protein assay. In mice experiments, livers were homogenized in PBS and 100 $\mu$l of the homogenate was used for extraction of lipids. Total protein was measured with protein assay reagents from Bio-Rad (Richmond, CA, USA).

**Hepatic Level of Thiobarbituric Acid-Reactive Substances (TBARS).** The hepatic level of TBARS was measured using an OXI-TEK TBARS Assay Kit (Zeptometrix Corporation, New York, USA). Briefly, 100 mg of liver tissue was homogenized in 10 vol of normal saline. Then 100 $\mu$l of SDS and 2.5 ml of TBA/buffer reagent were added to 100 $\mu$l of this homogenate or the malondialdehyde standard. Samples were incubated at 95°C for 60 min, cooled in an ice bath for 10 min, and centrifuged at 3000 rpm for 15 min, after which the supernatant was analyzed by spectrophotometry (532 nm).

**Extraction of RNA and RT-PCR.** The medium was removed and the cells were washed twice with PBS. After centrifugation, total RNA was isolated using an RNeasy Mini Kit (Qiagen, Tokyo). From mouse, 20 mg of liver tissue was used for RNA extraction. Then 2 $\mu$g of total RNA was employed for reverse transcription using random hexamers (final concentration: 2.5 $\mu$M) and murine leukemia virus reverse transcriptase (final concentration: 2.5 U/$\mu$l) (Roche, Tokyo). Specific primer sets were synthesized for performance of the PCR (Table 1) and were used for assessment of liver-predominant mitochondrial carnitine palmitoyl transferase-1 (CPT1A in humans and CPT1 in mice; the rate-limiting enzyme of mitochondrial $\beta$-oxidation), acyl-CoA oxidase (ACO1 in humans and AOX in mice: the rate-limiting enzyme of peroxisomal $\beta$-oxidation), cytochrome P-450 4A11 (CYP4A11; involved in microsomal $\omega$-oxidation), multidrug resistance protein 3 (MDR3 in humans and Mdr2 in mice; an ABC transporter and phospholipid flippase), microsomal TG transfer protein (MTP: a vital protein for TG incorporation into VLDL), and two nuclear receptors (peroxisome proliferator-activated receptor $\alpha$[PPAR$\alpha$]] and peroxisome proliferator-activated receptor $\gamma$ (PPAR$\gamma$). Roles of these genes are summarized in Table 2. Amplification involved 30 cycles of denaturation at 95°C for 60 sec, annealing at each specified temperature (Table 1) for 30 sec, and extension at 72°C for 60 sec. The reaction products were analyzed on a 2% agarose gel and were visualized by ethidium bromide staining. The PCR products were excised from the gel, purified using a gel purification kit (Qiagen), and quantified by spectrophotometry. Dilutions

TABLE 1. PRIMER SETS IN THE EXPERIMENTS

| | *Forward* | *Reverse* | *Annealing temp. (°C)* |
|---|---|---|---|
| Human | | | |
| GAPDH | GAACGGGAAGCTCACTGGCATGGC | TGAGGTCCACCCTGTTGCTG | 65 |
| PPARα | GGAAAGCCCACTCTGCCCCCT | AGTCACCGAGGAGGGGCTCGA | 63 |
| PPARγ | CATTCTGGCCCACCAACTTTGG | TGGAGATGCAGGCTCCACTTTG | 63 |
| MDR3 (ABCB4) | GATGAAAAGGCTGCCACTAG | TTGCACTTCTGCTGCTTCAC | 62 |
| MTP | GGCTAGCCTATTTCAGACACA | GATGAGCCTGGTAGGTCACT | 60 |
| CPT1A | AGACGGTGGAACAGAGGCTGAAG | TGAGACCAAACAAAGTGATGATGTCAG | 67 |
| ACO1 | GGGCATGGCTATTCTCATTGC | CGAACAAGGTCAACAGAAGTTAGGTTC | 60 |
| CYP4A11 | GTGGCCCAACCCAGAGGT | TCCCAATGCAGTTCCTTGATC | 55 |
| Mouse | | | |
| GAPDH | AGAACATCCCTGCATCC | TTGTCATTGAGAGCAATGCC | 56 |
| PPARα | TGCAGAGCAACCATCCAG | TAATGGCGAATTATAAAC | 50 |
| PPARγ | GGTGAAACTCTGGGAGATTC | CAACCATTGGGTCAGCTCTT | 59 |
| Mdr2 (Abcb4) | TATCCGCTATGGCCGTGGGAA | ATCGGTGAGCTATCACAATGG | 56 |
| MTP | TGAGCGGCTATACAAGCTCAC | CTGGAAGATGCTCTTCTCGC | 60 |
| LCPT | CGCACGGAAGGAAAATGG | TGTGCCCAATATTCCTGG | 52 |
| AOX | CTTGTTCGCGCAAGTGAGG | CAGGATCCGACTGTTTACC | 56 |

ranging from $3 \times 10^{-5}$ to $3 \times 10^{2}$ pg were prepared in water and used as the standards.

**Quantitative PCR.** Quantitative PCR was performed using the Light-Cycler Fast-Start DNA Master SYBR Green system (Roche Molecular Biochemicals, Tokyo). PCR was carried out in a final reaction volume of 20 μl using 1 μl of each primer at 10 μM (final concentration: 0.5 μM), 1.6 μl of 25 mM $MgCl_2$(final concentration: 3 mM), 2 μl of the enzyme mix supplied, 12.4 μl of $H_2O$, and 2 μl of the template. The enzyme mix contained the reaction buffer, Fast-Start Taq DNA polymerase, and DNA double strand-specific SYBR Green I dye for detection of PCR products. PCR was performed in a Light-Cycler (Roche) with preincubation for 10 min at 95°C followed by 40 cycles of denaturation for 15 sec at 95°C, annealing for 5 sec at each specified temperature (see Table 1), and extension for 25 sec at 72°C, with fluorescent detection at the end of extension. Next, the PCR products were subjected to melting curve analysis to exclude the amplification of primer dimmers or other nonspecific products. If primer dimmers and nonspecific bands were detected, fluorescence detection was repeated after extension at each specified temperature for 1 sec. Analysis was carried out with Light-Cycler 3.5 software (Roche). Quantification was done using the "point fitting" mode and baseline adjustment. The standard curve for each gene was created using five different dilutions. The plot of the number of PCR cycles versus log concentration was considered reliable when the error was <0.2.

**Statistical Analysis.** Results are expressed as the mean ± SE. Statistical analysis was performed using Student's *t*-test, and $P < 0.05$ was defined as indicating significance.

## RESULTS

**HCV Core Protein Expression in HepG2 Cells.** The transfection efficiency of pCAG-LacZ was about 20%. HCV core protein expression by the cells was confirmed using the HCV core antigen ELISA. No HCV core antigen was detected in mock-transfected and nontransfected cells. The level of HCV core protein expression showed no difference between 24 and 48 hr after transfection (24 hr,

TABLE 2. ROLES OF ANALYZED GENES IN FATTY ACID METABOLISM

| | |
|---|---|
| MDR3 | Multidrug resistance protein 3<br>An ABC transporter and phospholipid flippase<br>*Role: Phospholipid secretion into bile* |
| MTP | Microsomal triglyceride transfer protein<br>A vital protein for TG incorporation into VLDL<br>*Role: triglyceride secretion into blood* |
| CPT1A | Liver-predominant mitochondrial carnitine palmitoyl transferase-1<br>The rate-limiting enzyme of mitochondrial β-oxidation<br>*Role: Fatty acid β-oxidation in the liver* |
| ACO1 | Acyl-CoA oxidase<br>The rate-limiting enzyme of peroxisomal β-oxidation<br>*Role: Fatty acid β-oxidation in the liver* |
| PPARα | Peroxisome proliferator-activated receptor α<br>A nuclear receptor<br>*Role: A nuclear receptor controlling lipid metabolism-associated genes* |
| PPARγ | Peroxisome proliferator-activated receptor γ<br>A nuclear receptor<br>*Role: A nuclear receptor controlling lipid metabolism-associated genes* |

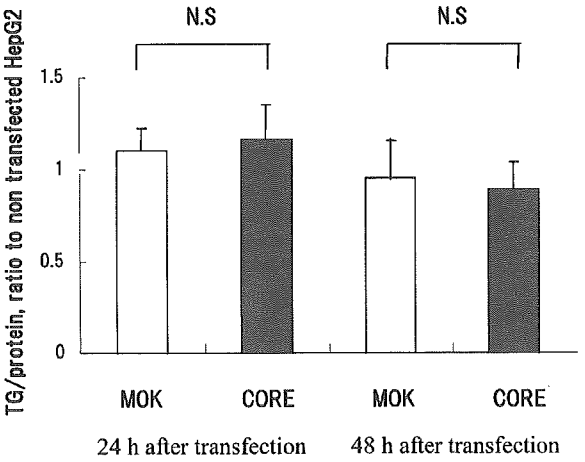


**Fig 2.** Effect of HCV core protein expression on cellular triglyceride (TG) content. Four micrograms of pCAG-MOK (control) or pCAG-HCVcore was transfected into HepG2 cells cultured in six-well plates by the lipofection method. At 24 or 48 hr after transfection, cells were collected for protein assay and lipid extraction. TG content was measured and expressed as the ratio to the protein content. Data are shown as values relative to those for nontransfected HepG2 cells. Each data point represents the mean ± SD of six individual experiments. $P$ = NS compared with pCAG-MOK (Student's $t$-test).

1.31 ± 0.20 nmol/mg protein; 48 hr, 1.25 ± 0.16 nmol/mg protein).

**TG Content of HepG2 Cells.** The cellular TG content at 24 hr after transfection showed no difference between HCV core transfectants (CORE) and mock transfectants (MOK) as control (CORE, 1.16 ± 0.19; MOK, 1.10 ± 0.13; $P = 0.57$). At 48 hr after transfection, the TG content also showed no difference between the groups (CORE, 0.88 ± 0.16; MOK, 0.95 ± 0.18; $P = 0.55$). Data are expressed as the ratio to nontransfected cells (Figure 2).

**Expression of Target Genes by HepG2 Cells.** At 24 hr after transfection, HCV CORE showed increased expression of mRNA for PPAR $\gamma$ (CORE, 2.39 ± 0.26; MOK, 1.98 ± 0.28; $P = 0.025$), MDR3 (CORE, 1.30 ± 0.21; MOK, 1.02 ± 0.20; $P = 0.030$), MTP (CORE, 0.37 ± 0.04; MOK, 0.26 ± 0.05; $P < 0.01$), and ACO1 (CORE, 1.11 ± 0.14; MOK, 0.76 ± 0.08; $P < 0.01$)gompared to MOK, while CPT (CORE, 1.18 ± 0.16; MOK, 0.94 ± 0.28; $P = 0.102$) and PPAR$\alpha$ (CORE, 0.84 ± 0.14; MOK, 0.69 ± 0.10; $P = 0.055$) expression was normal (Figure 3). At 48 hr after transfection, HCV CORE showed lower expression of mRNA for PPAR $\alpha$ (CORE, 0.89 ± 0.02; MOK, 0.96 ± 0.08;

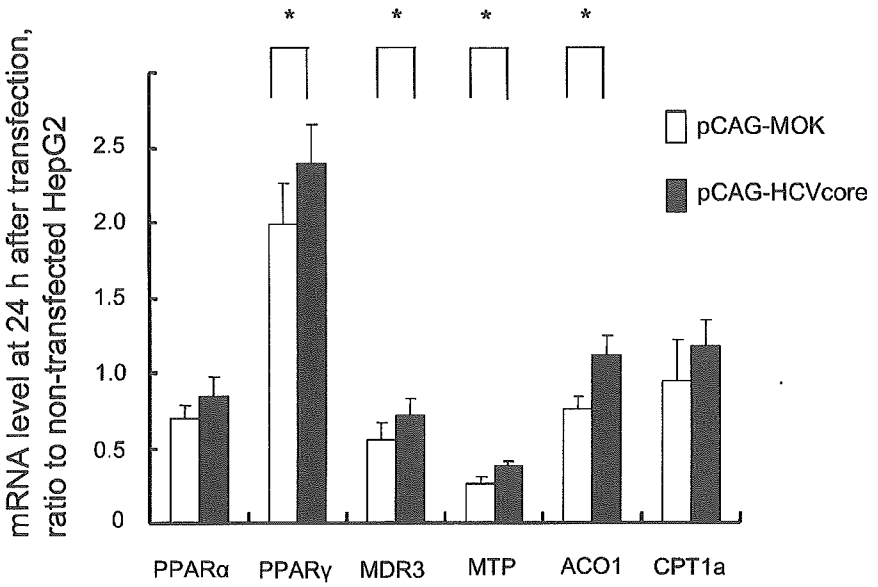


**Fig 3.** Effect of HCV core protein expression on mRNA levels at 24 hr after transfection. Three micrograms of pCAG-MOK (control) or pCAG-HCVcore was transfected into HepG2 cells cultured in 12-well plates by the lipofection method. At 24 hr after transfection, cells were collected for extraction of RNA. Complementary DNA was synthesized from 2 $\mu$g of RNA and used for quantified PCR with the Light-Cycler Fast-Start DNA Master SYBR Green system. GAPDH level was measured as the internal control, and the ratio to GAPDH was calculated for each sample. Data are shown as values relative to those for nontransfected HepG2 cells. Each data point represents the mean ± SD of 6 individual experiments. *$P < 0.05$ compared with pCAG-MOK (Student's $t$-test).

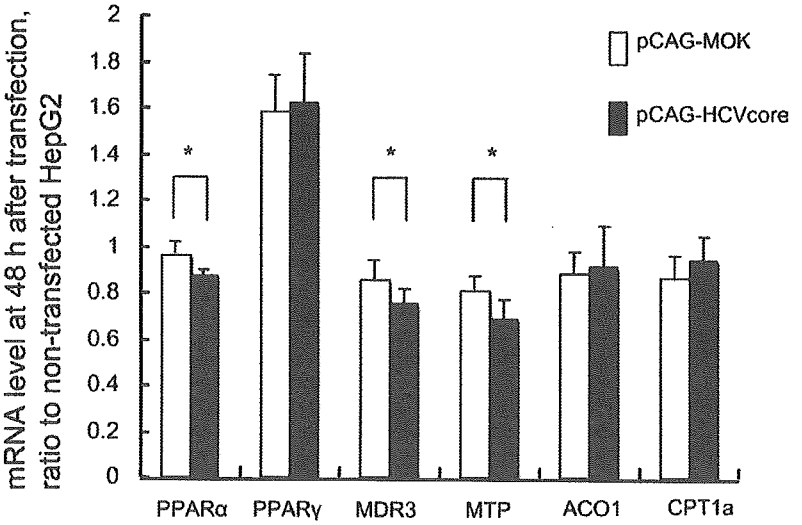


**Fig 4.** Effect of HCV core protein on mRNA expression at 48 hr after transfection. Three micrograms of pCAG-MOK (control) or pCAG-HCVcore was transfected into HepG2 cells cultured in 12-well plates by the lipofection method. At 48 hr after transfection, cells were collected and used for RNA extraction. Complementary DNA was synthesized from 2 $\mu$g of RNA and used for quantified PCR with the Light-Cycler Fast-Start DNA Master SYBR Green system. GAPDH was measured as an internal control, and the ratio to GAPDH was calculated for each sample. Data are shown as values relative to those for nontransfected HepG2 cells. Each data point represents the mean ± SD of 6 individual experiments. $*P < 0.05$ compared with pCAG-MOK (Student's $t$-test).

$P = 0.048$), MDR3 (CORE, 0.75 ± 0.06; MOK, 0.86 ± 0.08; $P = 0.031$), and MTP (CORE, 0.69 ± 0.08; MOK, 0.81 ± 0.07; $P = 0.016$) compared with MOK, while ACO1 returned to the control level (CORE, 0.91 ± 0.18; MOK, 0.88 ± 0.09; $P = 0.70$) and the CPT level was normal (CORE, 0.94 ± 0.13; MOK, 0.86 ± 0.10; $P = 0.27$). Data are expressed as the ratio to nontransfected cells (Figure 4). Experiments were repeated three times and similar results were obtained, with statistical significance. CYP4A11 was not detected by RT-PCR, so we could not make a standard for the Light-Cycler.

**HCV Core Protein Expression in Mice.** HCV core protein-expressing mice looked healthy and their body weight (BW) and liver weight remained within the normal range (BW [g]: PBS, 22.5 ± 0.816; AdexCAHCVcore (CORE), 21.7 ± 0.84; AdexCAlacZ (LacZ), as control, 21.5 ± 0.71). Similar mild elevation of ALT and mild hepatic lymphocyte infiltration were observed in both groups of adenovirus-infected mice, showing no differences between Core and LacZ (GPT [IU/ml]: PBS, 65 ± 17.8; CORE, 170 ± 59.4; LacZ, 142.5 ± 82.2). Lipid drops were not observed in either group (data not shown). Western blot analysis revealed the HCV core protein of about 19–20 kDa (Figure 5). In preliminary experiments, animals receiving an intravenous injection of $1 \times 10^9$ pfu developed severe hepatitis after 7 days, while animals receiving $1 \times 10^8$ pfu showed amild elevation of ALT, but their HCV core protein expression (based on quantification of mRNA and HCV core antigen) was significantly lower at 7 days after injection. Thus, we selected injection of $1 \times 10^9$ pfu and sacrifice at 3 days for the study protocol.

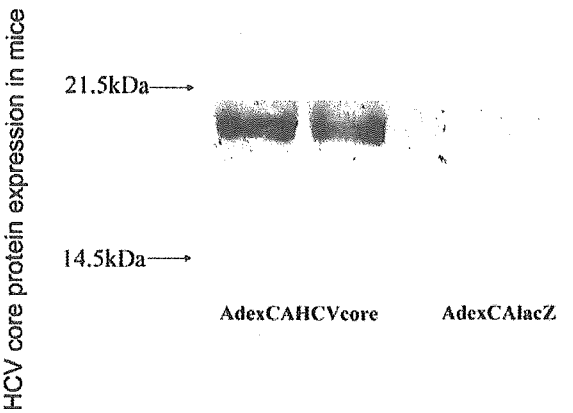


**Fig 5.** HCV core protein expression in mice. AdexCAlacZ (control recombinant adenovirus) or AdexCAHCVcore was used to infect male C57BL/6 mice (8–10 weeks old) by intravenous administration ($1 \times 10^9$ pfu). Three days after infection, livers were collected for protein assay. Using 50 $\mu$g of protein, HCV core protein expression was confirmed by Western blotting with a mouse monoclonal antibody for HCV core protein (19–20 kDa).

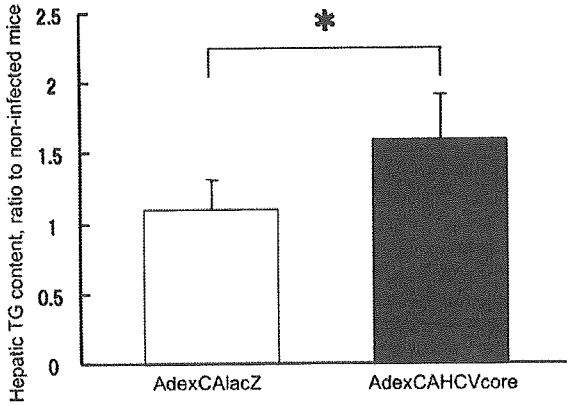


**Fig 6.** Effect of HCV core protein expression on the hepatic triglyceride content in mice. AdexCAlacZ (control adenovirus) or AdexCAHCVcore was used to infect male C57BL/6 mice (8–10 weeks old) by intravenous administration ($1 \times 10^9$ pfu). At 3 days after infection, the livers were collected and 100 $\mu$l of liver homogenate was used for lipid extraction and for the protein assay. The TG content was measured and expressed as the ratio to the protein content. Data are shown as values relative to those for noninfected mice. Each data point represents the mean ± SD of four individual mice. $^*P < 0.05$ compared with AdexCAlacZ (control adenovirus) by Student's $t$-test.

**Hepatic TG Level in Mice.** Animals injected with AdexCAHCVcore showed a 1.45-fold increase in hepatic TG content compared to animals injected with AdexCAlacZ (CORE, 1.60 ± 0.33; LacZ, 1.10 ± 0.21; $P = 0.044$; $N = 4$). Data are expressed as the ratio to noninfected mice (Figure 6).

**Expression of Target Genes in Mice.** In the livers of HCV core protein-expressing mice, PPAR $\alpha$ (CORE, 0.59 ± 0.11; LacZ, 1.33 ± 0.21; $P < 0.01$), PPAR $\gamma$ (CORE, 1.05 ± 0.10; LacZ, 2.43 ± 0.69; $P < 0.01$), Mdr2 (CORE, 0.85 ± 0.08; LacZ, 1.12 ± 0.12; $P = 0.011$), AOX (CORE, 0.235 ± 0.08; LacZ, 0.401 ± 0.07; $P = 0.02$), and CPT (CORE, 1.14 ± 0.14; LacZ 2.34 ± 0.51; $P < 0.01$) were all down-regulated, while the level of MTP mRNA was unchanged (CORE, 1.37 ± 0.08; LacZ, 1.24 ± 0.17; $P = 0.22$; $N = 4$). Data are expressed as the ratio to noninfected mice (Figure 7).

**Hepatic TBARS Level.** In the livers of HCV core protein-expressing mice, the TBARS level was increased compared with that in the control group (CORE, 0.84 ± 0.08; LacZ, 0.41 ± 0.01; $P < 0.01$; $N = 4$) (Figure 8).

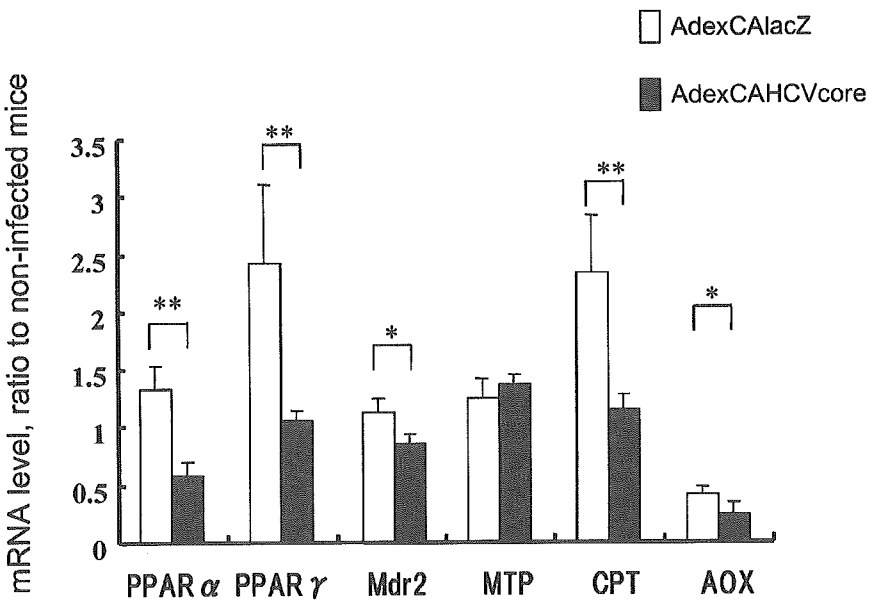


**Fig 7.** Effect of HCV core protein expression on mRNA levels in mice. AdexCAlacZ (control adenovirus) or AdexCAHCVcore was used to infect male C57BL/6 mice (8–10 weeks old) by intravenous administration ($1 \times 10^9$ pfu). At 3 days after infection, livers were collected for RNA extraction. Complementary DNA was synthesized from 2 $\mu$g of RNA and used for quantified PCR with the Light-Cycler Fast-Start DNA Master SYBR Green system. GAPDH was measured as an internal control, and the ratio to GAPDH was calculated for each sample. Data are shown as relative values to those for noninfected mice. Each data point represents the mean ± SD of four individual mice. $^*P < 0.05$ and $^{**}P < 0.01$ compared with AdexCAlacZ (control adenovirus) by Student's $t$-test.

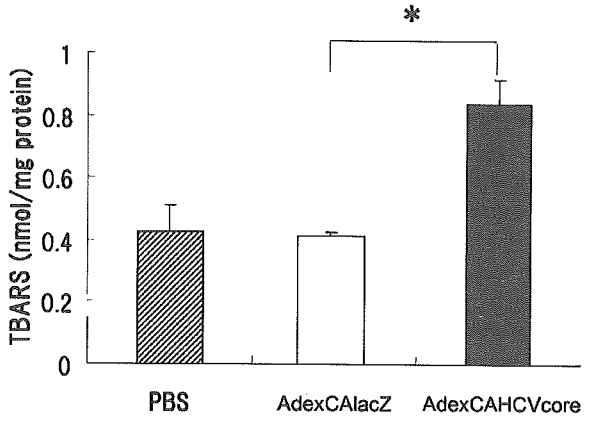


**Fig 8.** Effect of HCV core protein expression on TBARS in the mouse liver. AdexCAlacZ (control adenovirus) or AdexCAHCVcore was used to infect male C57BL/6 mice (8–10 weeks old) by intravenous administration ($1 \times 10^9$ pfu). At 3 days after infection, livers were homogenized in 10 vol of normal saline. TBARS and total protein (TP) levels were measured as described under Materials and Methods. Data are expressed as the ratio to the TP level. Each data point represents the mean ± SD of four individual mice. $^*P < 0.01$ compared with AdexCAlacZ (control adenovirus) by Student's $t$-test.

## DISCUSSION

HCV core protein was recently reported to cause hepatic steatosis and induction of reactive oxygen species (ROS) in an HCV core protein transgenic mouse model (18–20). In the transgenic mouse model, it was also shown that a decrease in MTP activity contributes to HCV core protein-related steatosis, while $\beta$-oxidation is unchanged (24), but the mechanism involved is still unclear. This study was the first investigation of the effect of HCV core protein on the expression of fatty acid metabolism-associated molecules in the acute expression mice model.

Hepatic accumulation of TG is principally driven by the following factors: (a) fatty acid overload (28, 29), (b) inhibition of fatty acid $\beta$-oxidation (28, 29), (c) decreased secretion of TG-rich very low density lipoprotein (VLDL) (28, 29), (d) increased de novo fatty acid synthesis, (e) decreased transformation to phospholipids, and (f) a combination of these mechanisms.

In the present study, we initially tested the effect of HCV core protein on a human cell line (HepG2). At 24 hr after transfection, the cellular TG level was unchanged, but the expression of several genes that are thought to promote fatty acid consumption (MTP, ACO1, and MDR3) was up-regulated. At 48 hr after transfection, there was either normal gene expression (ACO1) or a decrease in expression (PPAR$\alpha$, MDR3, and MTP). At 48 hr after transfection, the level of HCV core antigen was still the same as at 24 hr, so it seems possible that HCV core protein may act to down-regulate these genes over a longer period. To further evaluate the effects of HCV core protein, we performed in vivo experiments using transient expression of HCV core protein in mice. Although fatty change of the liver was not seen histologically, the hepatic TG level was increased by transient HCV core protein expression. In addition, expression of mRNA for all of the molecules investigated, except MTP, was down-regulated by HCV core protein expression. The mechanism involved is not understood at present, but reduced expression of these genes might contribute to hepatic TG accumulation.

CPT is the rate-limiting enzyme for mitochondrial $\beta$-oxidation (30), which is the main pathway of fatty acid consumption and ROS production. There was a recent report (20) that localization of HCV core protein in the mitochondria led to the increased production of ROS, decreased mitochondrial membrane permeability, and impairment of mitochondrial function. It remains unclear whether ROS induces fat accumulation or whether the accumulation of fat causes an increase in ROS, as well as whether decreased expression of CPT-1 is the first response to HCV core protein expression or follows other earlier changes. However, HCV core expression seems to contribute to hepatic accumulation of lipids and an increase in ROS in mice, along with reduced expression of various fatty acid metabolism-associated genes. AOX is vital for peroxisomal $\beta$-oxidation (30) and it has been reported that AOX knockout mice develop steatohepatitis, up-regulation of CYP4A gene expression, and increased production of ROS (31). We were unable to evaluate CYP4A11 in the present study, but the association of HCV-related steatosis with microsomal $\omega$-oxidation is interesting. Mdr2 (Abcb4) is a member of the Abcb subfamily of adenosine triphosphate-binding cassette (ABC) transporter proteins. Mdr2 Pgp is exclusively localized to the canalicular membrane and controls the secretion of phospholipids into the bile (32). We thought that impaired biliary phospholipid secretion might have a role in HCV-related steatosis, based on the fact that phospholipid-associated fatty acid secretion into bile (about 25 $\mu$mol per day) is substantial in relation to the hepatic amount of triglyceride-associated fatty acids (about 75 $\mu$mol) (33). We found that the expression of MDR3 and Mdr2 was down-regulated, suggesting that reduced expression of these genes could have a causative role in HCV-related steatosis.

Interestingly, down-regulation of Mdr2, AOX, and CPT in the mice was accompanied by down-regulation of PPAR$\alpha$. In mice, the other three genes are thought to undergo transcriptional regulation by PPAR$\alpha$ (33, 34), so their expression might be down-regulated secondary to the down-regulation of PPAR$\alpha$. HCV core protein is mainly

localized in the cytosol, but also exists in the nucleus (35, 36), so it is possible that this protein could influence gene transcription. Tsustumi *et al.* (37) used a luciferase assay to show that transcriptional activation of ACO-1 via PPRE is promoted at 24 hr after HCV core protein expression (23). However, we found down-regulation of target gene expression accompanied by decreased PPAR$\alpha$ expression after 3 days of HCV core protein expression in mice, as well as at 48 hr after transfection of cells. The expression of PPAR$\alpha$ was reported to be under transcriptional regulation by glucocorticoids (38), but the mechanism remains unclear. Accordingly, the mechanism leading to down-regulation of PPAR$\alpha$ after HCV core protein expression is also unclear. The lower expression of PPAR$\alpha$ and the genes it regulates in human hepatocytes than in mouse hepatocytes (39) could be a reason for the lack of an increase in TG and the small decline in gene expression in our cell experiment. Fibrates that bind with PPAR$\alpha$ and increase its activity (although not its expression) might be useful for controlling HCV-related steatosis by increasing the $\beta$-oxidation and bliary secretion of fatty acids.

PPAR$\gamma$ improves insulin resistance and is also reported to improve hepatic fibrosis and nonalcholic steatohepatitis (40, 41). Because PPAR$\gamma$ gene expression also showed down-regulation by HCV core protein expression in this study , it may be necessary to examine the role of glucose metabolism, de novo synthesis of fatty acids from glucose, and fatty acid flux through hepatocytes in HCV-related steatosis.

In this study, the increase in TBARS level was found in mice with transient expression of HCV core protein. This suggests that ROS production might be induced by HCV core protein expression, although no mechanistic information for this was provided in this study. It also remains unclear whether intrahepatic fat accumulation enhances ROS production as reflected by an increase in TBARS or, inversely, whether ROS production induces fatty liver change through ROS-associated mitochondrial dysfunction. Certainly, further investigations are needed to clarify this uncertainty, but the fact that HCV core protein expression in mice contributes to the increase in TBARS level may partially characterize the pathogenesis of HCV-related hepatic damage.

In summary, transient expression of HCV core protein in mice down-regulated the expression of various lipid metabolism-associated genes (Mdr2, CPT, and AOX). It also caused down-regulation of PPAR$\alpha$ expression and led to the accumulation of TG and the induction of oxidative stress. These findings may provide some clues to the understanding of HCV-related steatosis and to the induction of ROS production and carcinogenesis by infection with this virus.

## REFERENCES


1. Alter MJ, Margolis HS, Krawczynski K, Judson FN, Mares A, Alexander WJ, Hu PY, Miller JK, Gerber MA, Sampliner RE, Meeks EL, Beach MJ: The natural history of community-acquired hepatitis C in the United States. N Engl J Med 327:1899–1905,1992
2. Seeff LB, Buskell-Bales Z, Wright EC, Durako SJ, Alter HJ, Iber FL, Hollinger FB, Gitnick G, Knodell RG, Perrillo RP, Steevens CE, Hollingworth CG, NHLBI study Group: Long-term mortality after transfusion-associated non-A, non-B hepatitis. N Engl J Med 327:1906–1911, 1992
3. Seeff LB: Natural history of hepatitis C. Hepatology 26:21S–28S, 1997
4. Koziel MJ, Dudley D, Wong JT, Dienstag J, Houghton M, Ralston R, Walker BD: Intrahepatic cytotoxic T lymphocytes specific for hepatitis C virus in persons with chronic hepatitis. J Immunol 149:3339–3344, 1992
5. Cerny A, Chisari FV: Pathogenesis of chronic hepatitis C: immunological features of hepatic injury and viral persistence. Hepatology 30:595–601, 1999
6. Rubbia-Brandt L, Quadri R, Abid K, Giostra E, Male PJ, Mentha G, Spahr L, Zarski JP, Borisch B, Hadengue A, Negro F: Hepatocyte steatosis is a cytopathic effect of hepatitis C virus genotype 3. J Hepatol 33:106–115, 2000
7. Scheuer PJ, Davies SE, Dhillon AP: Histopathological aspects of viral hepatitis. J Viral Hepat 3:277–283, 1996
8. Fujie H, Yotsuyanagi H, Moriya K, Shintani Y, Tsutsumi T, Takayama T, Makuuchi M, Matsuura Y, Miyamura T, Kimura S, Koike K: Steatosis and intrahepatic hepatitis C virus in chronic hepatitis. J Med Virol 59:141–145, 1999
9. Goodman ZD, Ishak KG: Histopathologic findings in chronic hepatitis C virus infection. Semin Liver Dis 15:70–81, 1995
10. Barba G, Harper F, Harada T, Kohara M, Goulinet S, Matsuura Y, Eder G, Schaff Z, Chapman MJ, Miyamura T, Brechot C: Hepatitis C virus core protein shows a cytoplasmic localization and associates to cellular lipid storage droplets. Proc Natl Acad Sci USA 94:1200–1205, 1997
11. Ray RB, Lagging LM, Meyer K, Ray R: Hepatitis C virus core protein cooperates with ras and transforms primary rat embryo fibroblasts to tumorigenic phenotype. J Virol 70:4438–4443, 1996
12. Ray RB, Meyer K, Ray R: Suppression of apoptotic cell death by hepatitis C virus core protein. Virology 226:176–182, 1996
13. Zhu N, Khoshnan A, Schneider R, Matsumoto M, Dennert G, Ware C, Lai MM: Hepatitis C virus core protein binds to the cytoplasmic domain of tumor necrosis factor (TNF) receptor 1 and enhances TNF-induced apoptosis. J Virol 72:3691–3697, 1998
14. Honda M, Kaneko S, Shimazaki T, Matsushita E, Kobayashi K, Ping LH, Zhang HC, Lemon SM: Hepatitis C virus core protein induces apoptosis and impairs cell-cycle regulation in stably transformed Chinese hamster ovary cells. Hepatology 31:1351–1359, 2000
15. Sakamuro D, Furukawa T, Takegami T. Sakamuro D, Furukawa T, Takegami T: Hepatitis C virus nonstructural protein NS3 transforms NIH 3T3 cells. J Virol 69:3893–3896, 1995
16. McLauchlan J, Lemberg MK, Hope G, Martoglio B: Intramembrane proteolysis promotes trafficking of hepatitis C virus core protein to lipid droplets. EMBO J 21:3980–3988, 2002
17. Shi ST, Polyak SJ, Tu H, Taylor DR, Gretch DR, Lai MM: Hepatitis C virus NS5A colocalizes with the core protein on lipid droplets and interacts with apolipoproteins. Virology 292:198–210, 2002
18. Moriya K, Yotsuyanagi H, Shintani Y, Fujie H, Ishibashi K, Matsuura Y, Miyamura T, Koike K: Hepatitis C virus core protein

induces hepatic steatosis in transgenic mice. J Gen Virol 78:1527–1531, 1997
19. Lerat H, Honda M, Beard MR, Loesch K, Sun J, Yang Y, Okuda M, Gosert R, Xiao SY, Weinman SA, Lemon SM: Steatosis and liver cancer in transgenic mice expressing the structural and nonstructural proteins of hepatitis C virus. Gastroenterology 122:352–365, 2002
20. Okuda M, Li K, Beard MR, Showalter LA, Scholle F, Lemon SM, Weinman SA: Mitochondrial injury, oxidative stress, and antioxidant gene expression are induced by hepatitis C virus core protein. Gastroenterology 122:366–375, 2002
21. Moriya K, Nakagawa K, Santa T, Shintani Y, Fujie H, Miyoshi H, Tsutsumi T, Miyazawa T, Ishibashi K, Horie T, Imai K, Todoroki T, Kimura S, Koike K: Oxidative stress in the absence of inflammation in a mouse model for hepatitis C virus-associated hepatocarcinogenesis. Cancer Res 61:4365–4370, 2001
22. Moriya K, Fujie H, Shintani Y, Yotsuyanagi H, Tsutsumi T, Ishibashi K, Matsuura Y, Kimura S, Miyamura T, Koike K: The core protein of hepatitis C virus induces hepatocellular carcinoma in transgenic mice. Nat Med 4:1065–1067, 1998
23. Sabile A, Perlemuter G, Bono F, Kohara K, Demaugre F, Kohara M, Matsuura Y, Miyamura T, Brechot C, Barba G: Hepatitis C virus core protein binds to apolipoprotein AII and its secretion is modulated by fibrates. Hepatology 30:1064–1076, 1999
24. Perlemuter G, Sabile A, Letteron P, Vona G, Topilco A, Chretien Y, Koike K, Pessayre D, Chapman J, Barba G, Brechot C: Hepatitis C virus core protein inhibits microsomal triglyceride transfer protein activity and very low density lipoprotein secretion: a model of viral-related steatosis. FASEB J 16:185–194, 2002
25. Miyake S, Makimura M, Kanegae Y, Harada S, Sato Y, Takamori K, Tokuda C, Saito I: Efficient generation of recombinant adenoviruses using adenovirus DNA-terminal protein complex and a cosmid bearing the full–length virus genome. Proc Natl Acad Sci USA 93:1320–1324, 1996
26. Kanegae Y, Lee G, Sato Y, Tanaka M, Nakai M, Sakaki T, Sugano S, Saito I: Efficient gene activation in mammalian cells by using recombinant adenovirus expressing site-specific Cre recombinase. Nucleic Acids Res 23:3816–3821, 1995
27. Bligh EG, Dyer WJ: A rapid method of total lipid extraction and purification. Can J Med Sci 37:911–917, 1959
28. Day CP, James OF: Hepatic steatosis: Innocent bystander or guilty party? Hepatology 27:1463–1466, 1988
29. Fong DG., Nehra V, Lindor KD, Buchman AL: Metabolic and nutritional considerations in nonalcoholic fatty liver. Hepatology 32:3–10, 2000
30. Reddy JK: Nonalcoholic steatosis and steatohepatitis. III. Peroxisomal beta-oxidation, PPAR alpha, and steatohepatitis. Am J Physiol Gastrointest Liver Physiol. 281:G1333–G1339, 2001 (review)
31. Fan C, Pan J, Chu R, Lee D, Kluckman KD, Usuda N, Singh I, *et al.*: Hepatocellular and hepatic peroxisomal alternation in mice with a disrupted peroxisomal fatty acyl–coenzyme A oxidase gene. J Biol Chem 271:24698–24710, 1996
32. Smit JJ, Schinkel AH: Homozygous disruption of the murine mdr2 P-glycoprotein gene leads to a complete absense of phospholipid from bile and to liver desease. Cell 75:451–462, 1993
33. Kok T, Wolters H, Bloks V, Havinga R, Jansen P, Ataels B, Kuipers F: Induction of hepatic ABC transporter expression is part of the PPAR$\alpha$-mediated fasting response in the mouse. Gastroenterology 124:160–171, 2002
34. Duplus E, Forest C: Is there a single mechanism for fatty acid regulation of gene transcription? Biochem Pharmacol 64:893–901, 2002 (review)
35. Moriya K, Fujie H, Shintani Y, Yotsuyanagi H, Tsutsumi T, Ishibashi K, Matsuura Y, Kimura S, Miyamura T, Koike K: The core protein of hepatitis C virus induces hepatocellular carcinoma in transgenic mouse. Nat Med 4:1065–1067, 1998
36. Yasui K: The native form and maturation process of hepatitis C virus core protein. J Virol 72:6048–6055, 1998
37. Tsutsumi T, Suzuki T, Shimoike T, Suzuki R, Moriya K, Shintani Y, Fujii H, Matsuura Y, Koike K, Miyamura T: Interaction of hepatitis C virus core protein with retinoid X receptor $\alpha$ modulates its transcriptional activity. Hepatology 35:937–946, 2002
38. Lemberger T, Saladin R, Vazquez M, Assimacopoulos F, Staels B, Desvergne B, Wahli W, Auwerx J: Expression of the peroxisome proliferators-activated receptor alpha gene is stimulated by stress and follows a diurnal rhythm. J Biol Chem. 19:1764–1769, 1996
39. Hsu M, Savas U, Griffin K, Johnson E: Identification of peroxisome proliferators-responsive human genes by elevated expression of peroxisome proliferators-activated receptor $\alpha$ in HepG2 Cells. J. Biol. Chem 276:27950–27958, 2001
40. Neuschwander-Tetri BA, Brunt EM, Wehmeier KR, Oliver D, Bacon BR: Improved nonalcoholic steatohepatitis after 48 weeks of treatment with the PPAR-gamma ligand rosiglitazone. Hepatology 38:1008–1017, 2003
41. Alter MJ, Margolis HS, Krawczynski K, Judson FN, Mares A, Alexander WJ, Hu PY, Miller JK, Gerber MA, Sampliner RE, Meeks EL, Beach MJ: The natural history of community-acquired hepatitis C in the United States. N Engl J Med 327:1899–1905,1992
42. Seeff LB, Buskell–Bales Z, Wright EC, Durako SJ, Alter HJ, Iber FL, Hollinger FB, Gitnick G, Knodell RG, Perrillo RP, Steevens CE, Hollingworth CG, NHLBI study Group: Long-term mortality after transfusion-associated non-A, non-B hepatitis. N Engl J Med 327:1906–1911, 1992
43. Seeff LB: Natural history of hepatitis C. Hepatology 26:21S–28S, 1997
44. Koziel MJ, Dudley D, Wong JT, Dienstag J, Houghton M, Ralston R, Walker BD: Intrahepatic cytotoxic T lymphocytes specific for hepatitis C virus in persons with chronic hepatitis. J Immunol 149:3339–3344, 1992
45. Cerny A, Chisari FV: Pathogenesis of chronic hepatitis C: immunological features of hepatic injury and viral persistence. Hepatology 30:595–601, 1999
46. Rubbia-Brandt L, Quadri R, Abid K, Giostra E, Male PJ, Mentha G, Spahr L, Zarski JP, Borisch B, Hadengue A, Negro F: Hepatocyte steatosis is a cytopathic effect of hepatitis C virus genotype 3. J Hepatol 33:106–115, 2000
47. Scheuer PJ, Davies SE, Dhillon AP: Histopathological aspects of viral hepatitis. J Viral Hepat 3:277–283, 1996
48. Fujie H, Yotsuyanagi H, Moriya K, Shintani Y, Tsutsumi T, Takayama T, Makuuchi M, Matsuura Y, Miyamura T, Kimura S, Koike K: Steatosis and intrahepatic hepatitis C virus in chronic hepatitis. J Med Virol 59:141–145, 1999
49. Goodman ZD, Ishak KG: Histopathologic findings in chronic hepatitis C virus infection. Semin Liver Dis 15:70–81, 1995
50. Barba G, Harper F, Harada T, Kohara M, Goulinet S, Matsuura Y, Eder G, Schaff Z, Chapman MJ, Miyamura T, Brechot C: Hepatitis C virus core protein shows a cytoplasmic localization and associates to cellular lipid storage droplets. Proc Natl Acad Sci USA 94:1200–1205, 1997
51. Ray RB, Lagging LM, Meyer K, Ray R: Hepatitis C virus core protein cooperates with ras and transforms primary rat embryo fibroblasts to tumorigenic phenotype. J Virol 70:4438–4443, 1996
52. Ray RB, Meyer K, Ray R: Suppression of apoptotic cell death by hepatitis C virus core protein. Virology 226:176–182, 1996

53. Zhu N, Khoshnan A, Schneider R, Matsumoto M, Dennert G, Ware C, Lai MM: Hepatitis C virus core protein binds to the cytoplasmic domain of tumor necrosis factor (TNF) receptor 1 and enhances TNF-induced apoptosis. J Virol 72:3691–3697, 1998
54. Honda M, Kaneko S, Shimazaki T, Matsushita E, Kobayashi K, Ping LH, Zhang HC, Lemon SM: Hepatitis C virus core protein induces apoptosis and impairs cell-cycle regulation in stably transformed Chinese hamster ovary cells. Hepatology 31:1351–1359, 2000
55. Sakamuro D, Furukawa T, Takegami T. Sakamuro D, Furukawa T, Takegami T: Hepatitis C virus nonstructural protein NS3 transforms NIH 3T3 cells. J Virol 69:3893–3896, 1995
56. McLauchlan J, Lemberg MK, Hope G, Martoglio B: Intramembrane proteolysis promotes trafficking of hepatitis C virus core protein to lipid droplets. EMBO J 21:3980–3988, 2002
57. Shi ST, Polyak SJ, Tu H, Taylor DR, Gretch DR, Lai MM: Hepatitis C virus NS5A colocalizes with the core protein on lipid droplets and interacts with apolipoproteins. Virology 292:198–210, 2002
58. Moriya K, Yotsuyanagi H, Shintani Y, Fujie H, Ishibashi K, Matsuura Y, Miyamura T, Koike K: Hepatitis C virus core protein induces hepatic steatosis in transgenic mice. J Gen Virol 78:1527–1531, 1997
59. Lerat H, Honda M, Beard MR, Loesch K, Sun J, Yang Y, Okuda M, Gosert R, Xiao SY, Weinman SA, Lemon SM: Steatosis and liver cancer in transgenic mice expressing the structural and nonstructural proteins of hepatitis C virus. Gastroenterology 122:352–365, 2002
60. Okuda M, Li K, Beard MR, Showalter LA, Scholle F, Lemon SM, Weinman SA: Mitochondrial injury, oxidative stress, and antioxidant gene expression are induced by hepatitis C virus core protein. Gastroenterology 122:366–375, 2002
61. Moriya K, Nakagawa K, Santa T, Shintani Y, Fujie H, Miyoshi H, Tsutsumi T, Miyazawa T, Ishibashi K, Horie T, Imai K, Todoroki T, Kimura S, Koike K: Oxidative stress in the absence of inflammation in a mouse model for hepatitis C virus-associated hepatocarcinogenesis. Cancer Res 61:4365–4370, 2001
62. Moriya K, Fujie H, Shintani Y, Yotsuyanagi H, Tsutsumi T, Ishibashi K, Matsuura Y, Kimura S, Miyamura T, Koike K: The core protein of hepatitis C virus induces hepatocellular carcinoma in transgenic mice. Nat Med 4:1065–1067, 1998
63. Sabile A, Perlemuter G, Bono F, Kohara K, Demaugre F, Kohara M, Matsuura Y, Miyamura T, Brechot C, Barba G: Hepatitis C virus core protein binds to apolipoprotein AII and its secretion is modulated by fibrates. Hepatology 30:1064–1076, 1999
64. Perlemuter G, Sabile A, Letteron P, Vona G, Topilco A, Chretien Y, Koike K, Pessayre D, Chapman J, Barba G, Brechot C: Hepatitis C virus core protein inhibits microsomal triglyceride transfer protein activity and very low density lipoprotein secretion: a model of viral-related steatosis. FASEB J 16:185–194, 2002
65. Miyake S, Makimura M, Kanegae Y, Harada S, Sato Y, Takamori K, Tokuda C, Saito I: Efficient generation of recombinant adenoviruses using adenovirus DNA-terminal protein complex and a cosmid bearing the full–length virus genome. Proc Natl Acad Sci USA 93:1320–1324, 1996
66. Kanegae Y, Lee G, Sato Y, Tanaka M, Nakai M, Sakaki T, Sugano S, Saito I: Efficient gene activation in mammalian cells by using recombinant adenovirus expressing site-specific Cre recombinase. Nucleic Acids Res 23:3816–3821, 1995
67. Bligh EG, Dyer WJ: A rapid method of total lipid extraction and purification. Can J Med Sci 37:911–917, 1959
68. Day CP, James OF: Hepatic steatosis: Innocent bystander or guilty party? Hepatology 27:1463–1466, 1988
69. Fong DG., Nehra V, Lindor KD, Buchman AL: Metabolic and nutritional considerations in nonalcoholic fatty liver. Hepatology 32:3–10, 2000
70. Reddy JK: Nonalcoholic steatosis and steatohepatitis. III. Peroxisomal beta-oxidation, PPAR alpha, and steatohepatitis. Am J Physiol Gastrointest Liver Physiol. 281:G1333–G1339, 2001 (review)
71. Fan C, Pan J, Chu R, Lee D, Kluckman KD, Usuda N, Singh I, *et al.*: Hepatocellular and hepatic peroxisomal alternation in mice with a disrupted peroxisomal fatty acyl–coenzyme A oxidase gene. J Biol Chem 271:24698–24710, 1996
72. Smit JJ, Schinkel AH: Homozygous disruption of the murine mdr2 P-glycoprotein gene leads to a complete absense of phospholipid from bile and to liver desease. Cell 75:451–462, 1993
73. Kok T, Wolters H, Bloks V, Havinga R, Jansen P, Ataels B, Kuipers F: Induction of hepatic ABC transporter expression is part of the PPAR$\alpha$-mediated fasting response in the mouse. Gastroenterology 124:160–171, 2002
74. Duplus E, Forest C: Is there a single mechanism for fatty acid regulation of gene transcription? Biochem Pharmacol 64:893–901, 2002 (review)
75. Moriya K, Fujie H, Shintani Y, Yotsuyanagi H, Tsutsumi T, Ishibashi K, Matsuura Y, Kimura S, Miyamura T, Koike K: The core protein of hepatitis C virus induces hepatocellular carcinoma in transgenic mouse. Nat Med 4:1065–1067, 1998
76. Yasui.K: The native form and maturation process of hepatitis C virus core protein. J Virol 72:6048–6055, 1998
77. Tsutsumi T, Suzuki T, Shimoike T, Suzuki R, Moriya K, Shintani Y, Fujii H, Matsuura Y, Koike K, Miyamura T: Interaction of hepatitis C virus core protein with retinoid X receptor $\alpha$ modulates its transcriptional activity. Hepatology 35:937–946, 2002
78. Lemberger T, Saladin R, Vazquez M, Assimacopoulos F, Staels B, Desvergne B, Wahli W, Auwerx J: Expression of the peroxisome proliferators-activated receptor alpha gene is stimulated by stress and follows a diurnal rhythm. J Biol Chem. 19:1764–1769, 1996
79. Hsu M, Savas U, Griffin K, Johnson E: Identification of peroxisome proliferators-responsive human genes by elevated expression of peroxisome proliferators-activated receptor $\alpha$ in HepG2 Cells. J. Biol. Chem 276:27950–27958, 2001
80. Neuschwander-Tetri BA, Brunt EM, Wehmeier KR, Oliver D, Bacon BR: Improved nonalcoholic steatohepatitis after 48 weeks of treatment with the PPAR-gamma ligand rosiglitazone. Hepatology 38:008–1017, 2003
81. Promrat K, Lutchman G, Uwaifo GI, Freedman RJ, Soza A, Heller T, Doo E, Ghany M, Premkumar A, Park Y, Liang TJ, Yanovski JA, Kleiner DE, Hoofnagle JH: A pilot study of pioglitazone treatment for nonalcoholic steatohepatitis. Hepatology 39:188–196, 2004

GASTROENTEROLOGY 2005;128:138–146

# Suppression of Macrophage Infiltration Inhibits Activation of Hepatic Stellate Cells and Liver Fibrogenesis in Rats

MICHIO IMAMURA,*,† TADASHI OGAWA,* YASUYUKI SASAGURI,§ KAZUAKI CHAYAMA,† and HIKARU UENO*

*Department of Biochemistry and Molecular Pathophysiology, University of Occupational and Environmental Health, School of Medicine, Kitakyushu, Japan; †Department of Medicine and Molecular Science, Graduate School of Biomedical Science, Hiroshima University, Hiroshima, Japan; and §Department of Pathology and Cell Biology, University of Occupational and Environmental Health, School of Medicine, Kitakyushu, Japan

***Background & Aims:*** **Monocytes/macrophages infiltrate into injured livers. We tried to clarify their roles in inflammation and subsequent fibrogenesis by inhibiting their infiltration with a mutated form (7ND; 7 amino acids at the N-terminal were deleted) of monocyte chemoattractant protein 1, which may function as a dominant-negative mutant.** ***Methods:*** **Rats were injected via the tail vein with an adenovirus expressing either human 7ND (Ad7ND), a truncated type II transforming growth factor β receptor (AdTβ-TR), which works as a dominant-negative receptor, bacterial β-galactosidase (AdLacZ), or saline. Seven days later, the rats were treated with dimethylnitrosamine for 1–21 days.** ***Results:*** **Within 24 hours after a single dimethylnitrosamine injection, macrophages were observed in livers. With a 3-day dimethylnitrosamine treatment, activated hepatic stellate cells were detectable in livers in AdLacZ-, AdTβ-TR–, and saline-injected rats. In contrast, in the Ad7ND-treated rats, infiltration of macrophages was markedly reduced, and activated hepatic stellate cells were not detectable. After a 3-week dimethylnitrosamine treatment, fibrogenesis was almost completely inhibited, and activated hepatic stellate cells were hardly seen in livers in both Ad7ND- and AdTβ-TR–treated rats.** ***Conclusions:*** **Our results show that blockade of macrophage infiltration inhibits activation of hepatic stellate cells and leads to suppression of liver fibrogenesis. The presence of activated hepatic stellate cells in the initial phase after injury and its absence at a later phase in the AdTβ-TR–treated livers indicate that transforming growth factor β is not an activating factor for hepatic stellate cells, and this suggests that transforming growth factor β is required for the survival of activated hepatic stellate cells. Our study suggests that infiltrated macrophages may themselves produce an activating factor for hepatic stellate cells.**

Inflammation is always accompanied by an infiltration by leukocytes,[1] a process that is thought to be regulated by chemotactic cytokines called *chemokines*.[1,2] Monocyte chemoattractant protein (MCP)-1, one of these chemokines, induces infiltration by monocytes/macrophages and lymphocytes[3] by binding to a specific receptor, CCR2.[1,2] In animal models of liver injury[4,5] and in patients with chronic hepatitis,[6,7] MCP-1 is detectable in both livers and serum. Injury-induced inflammation results in tissue remodeling or liver fibrosis. However, the actual roles performed by infiltrated monocytes/macrophages and MCP-1 in liver fibrogenesis are largely unknown.

During liver fibrogenesis, hepatic stellate cells (HSC) are activated to myofibroblast-like cells expressing α-actin. These activated HSC and myofibroblasts already existing in the portal field and around central veins may play a central role in fibrogenesis,[8] after which they produce extracellular matrix through the generation of various cytokines, including transforming growth factor (TGF)-β.[9] For fibrogenesis, HSC are considered to be the responsible cells, and TGF-β is one of the critical factors for fibrogenesis. In fact, when we inhibited the action of TGF-β by using a dominant-negative mutated receptor for TGF-β,[10] the activated HSC were markedly reduced in number, and fibrogenesis, as well as the progression of already-established fibrosis, was almost completely suppressed.[11–13] This shows the essential roles played by TGF-β and HSC in fibrotic remodeling after liver injury. However, the mechanism underlying the activation of HSC is not fully understood, although TGF-β has been believed to be an activating factor.[14]

In this study, to try to answer these questions, we introduced a mutated form of MCP-1 (7ND), which is

*Abbreviations used in this paper:* DMN, dimethylnitrosamine; ELISA, enzyme-linked immunosorbent assay; HSC, hepatic stellate cells; MCP, monocyte chemoattractant protein; MOI, multiplicity of infection; TGF, transforming growth factor; TUNEL, terminal deoxynucleotidyl transferase–mediated deoxyuridine triphosphate nick-end labeling.


0016-5085/05/$30.00
doi:10.1053/j.gastro.2004.10.005

considered to inhibit the action of MCP-1 as a dominant-negative mutant,[15,16] into dimethylnitrosamine (DMN)-treated rats, an established model of liver fibrosis with a pathology closely resembling that of human cirrhosis.[17,18] Some rats were given a dominant-negative TGF-β receptor to eliminate signaling by TGF-β.[11,12] We compared these rats in terms of (1) infiltration by monocytes/macrophages and activation of HSC, both of which occur in the acute phase after injury, and (2) fibrotic changes in the chronic phase after injury. Although inhibition of MCP-1 and blockade of TGF-β each led to a marked suppression of liver fibrogenesis, we were interested to find that some responses in the initial phase after injury were quite different between these 2 groups. Our study indicates that TGF-β is not an activating factor for HSC and suggests that infiltrated monocytes/macrophages may produce the activating factor(s).

## Materials and Methods

### Preparation of Adenoviruses

Replication-defective $E1^-$ and $E3^-$ adenoviral vectors expressing an amino-terminal deletion mutant of human MCP-1 (Ad7ND) with a FLAG epitope tag in its carboxyl-terminal (complementary DNA, a generous gift from Dr. B. Rollins, Harvard University),[15,16] a truncated human TGF-β type II receptor (AdTβ-TR),[10–12] or bacterial β-galactosidase (AdLacZ)[19] under a CA promoter comprising a cytomegalovirus enhancer and a chicken β-actin promoter[20] were prepared as previously described.[21]

### Detection of Mutated Human Monocyte Chemoattractant Protein 1 (7ND) and Rat Wild-Type Monocyte Chemoattractant Protein 1

COS cells were infected with either Ad7ND (multiplicity of infection [MOI] of 1, 10, and 100) or AdLacZ (MOI of 10), as previously described.[10] One day after infection, the medium was replaced with serum-free medium, and cells were incubated for a further 24 hours. A mutant MCP-1 (7ND) secreted into culture media was analyzed by Western blotting by using monoclonal antibodies against either FLAG (Abcam, Cambridge, UK) or human MCP-1 (Sanbio, 5400 AM Uden, The Netherlands), as previously described.[13]

7ND and rat MCP-1 were also detectable by enzyme-linked immunosorbent assay (ELISA). Livers were homogenized in phosphate-buffered saline with 1% Triton X-100, 0.1% sodium dodecyl sulfate, and 0.5% sodium deoxycholate. The homogenates were centrifuged at 20,000*g* for 30 minutes. 7ND and rat MCP-1 were measured in the supernatant of liver homogenates and in sera from rats by using a human MCP-1 ELISA kit (Biosource, Camarillo, CA) and a rat kit (Biosource), respectively, according to the manufacturer's instructions. These ELISA kits are species specific, and cross-reaction between human and rat MCP-1 is less than 5%. In fact, no human MCP-1 protein was detectable in samples from either intact or AdLacZ-infected rats (data not shown).

### Animal Models

All animals were treated under protocols approved by the institutional animal care committees, and the experiment was performed under both the institutional guidelines for animal experiments and by the Law (No. 105) and Notification (No. 6) of the Japanese government. Male Sprague–Dawley rats, 10 weeks old and weighing approximately 350 g, were given a single infusion of 0.5 mL of Ad7ND, AdTβ-TR, AdLacZ ($2 \times 10^9$ plaque-forming units per milliliter), or saline via the tail vein, as previously reported.[12] By this method, virtually all cells in the liver were infected and expressed the introduced molecule.[11,12] Seven days later, rats were given an intraperitoneal injection of DMN (10 μg/g body weight; Wako, Osaka, Japan) either once or at the indicated times (3 consecutive daily injections or 3 consecutive daily injections and 4 days off per week for 3 weeks), as previously reported.[11–13] After DMN treatment, blood was collected, and the rats were killed. Biochemical parameters were measured by using standard methods. The liver was either fixed with 4% buffered paraformaldehyde for histological examination or frozen immediately in liquid nitrogen for the extraction of hydroxyproline, the content of which was measured as described elsewhere.[22]

### Histological Examination

Liver sections were stained with hematoxylin or Masson trichrome or subjected to immunohistostaining by using antibodies against either CD68 (ED-1; Serotec, Raleigh, NC) or α-actin (Dako, Tokyo, Japan). Immunoreactive materials were visualized by using a streptavidin-biotin staining kit (Histofine SAB-PO kit; Nichirei, Tokyo, Japan) and diaminobenzidine. Macrophages (CD68-positive cells) and lymphocytes were counted by a technician blinded to the treatment regimen. Four random high-power (200×) fields from each section were examined. As negative controls, immunohistostaining was performed without the first antibodies.

### Determination of Hepatic Stellate Cells in Apoptosis

Fragmented DNA in apoptotic cells in liver sections was stained with diaminobenzidine (dark brown) by the terminal deoxynucleotidyl transferase–mediated deoxyuridine triphosphate nick-end labeling (TUNEL) technique by using a commercially available kit (Roche Diagnostics, Mannheim, Germany). Then, the sections were double-stained against α-actin and visualized with the aid of 3-amino-9-ethyl carbazole liquid substrate chromogen (red; Dako). As negative controls, the TUNEL reaction mixture was used without terminal transferase.


**Figure 1.** A mutated form of MCP-1 (7ND) is secreted from cells infected with Ad7ND. COS cells were infected either with Ad7ND or with AdLacZ at the indicated MOI. After 48 hours, the culture media were subjected to sodium dodecyl sulfate-polyacrylamide gel electrophoresis (12%) and analyzed by Western blotting by using antibodies against either (*A*) FLAG or (*B*) human MCP-1. Molecular markers are in kilodaltons.

### Statistical Analysis

Statistical analysis was performed by 1-way analysis of variance followed by Scheffé's test. $P < .05$ was considered significant.

## Results

### A Mutant Monocyte Chemoattractant Protein 1, 7ND, Was Secreted From Ad7ND-Infected Cells and Detected in the Serum and Liver of Ad7ND-Infected Rats

In the culture medium from Ad7ND-infected COS cells, 7ND was readily detectable in an MOI-dependent manner, as assessed by Western blotting analysis (Figure 1). Human 7ND and endogenous rat MCP-1 proteins were measured in sera (Figure 2*A*) and liver extracts (Figure 2*B*) from rats infected with Ad7ND. Seven days after gene transfer, a 3-week DMN treatment was begun. It is interesting to note that the amount of rat MCP-1 was not significantly changed by DMN treatment in either serum or liver. 7ND reached a peak on the seventh day after gene transfer and then declined gradually; however, the values were much higher than those obtained for rat MCP-1 in most time periods under DMN injury.

### Dimethylnitrosamine-Induced Infiltration by Macrophages and Lymphocytes and Activation of Hepatic Stellate Cells Were Both Suppressed in Ad7ND-Treated Livers

Rats were infused via the tail vein with either saline or an adenovirus expressing 1 of the following:

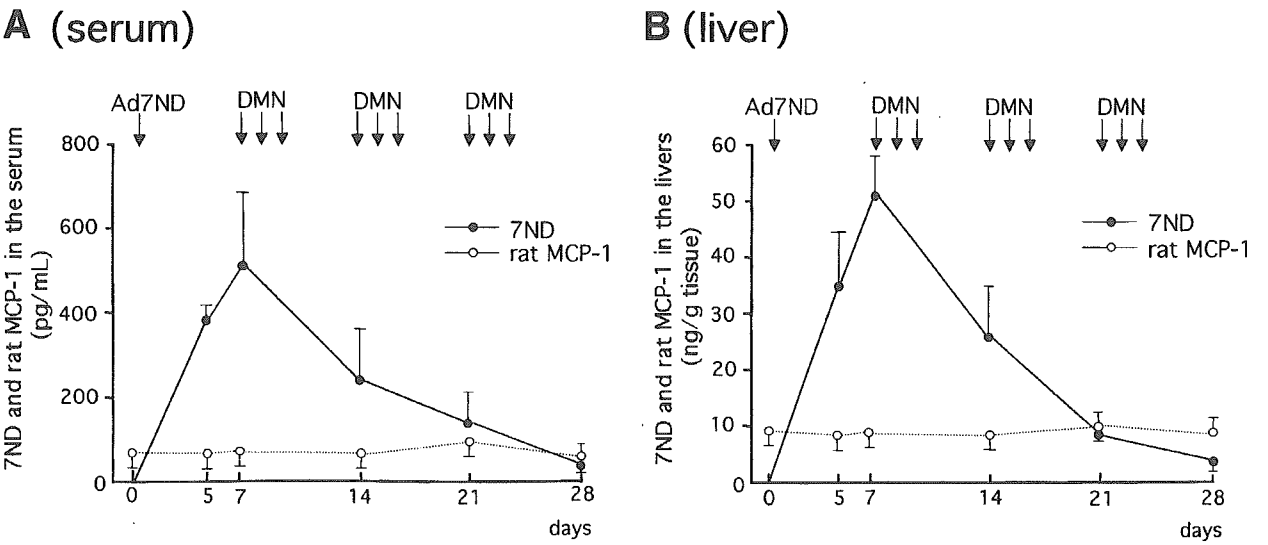


**Figure 2.** Amounts of human 7ND and rat MCP-1 in the sera (*A*) and livers (*B*) of DMN-injured rats. Rats were given a single infusion of Ad7ND (or saline infusion) via the tail vein. Seven days later, rats were subjected to a 3-week DMN treatment (shown as arrows). Rats were killed 5, 7 (just before the initiation of DMN treatment), 14, 21, and 28 days after Ad7ND injection. Means ± SD (n = 4) are shown.

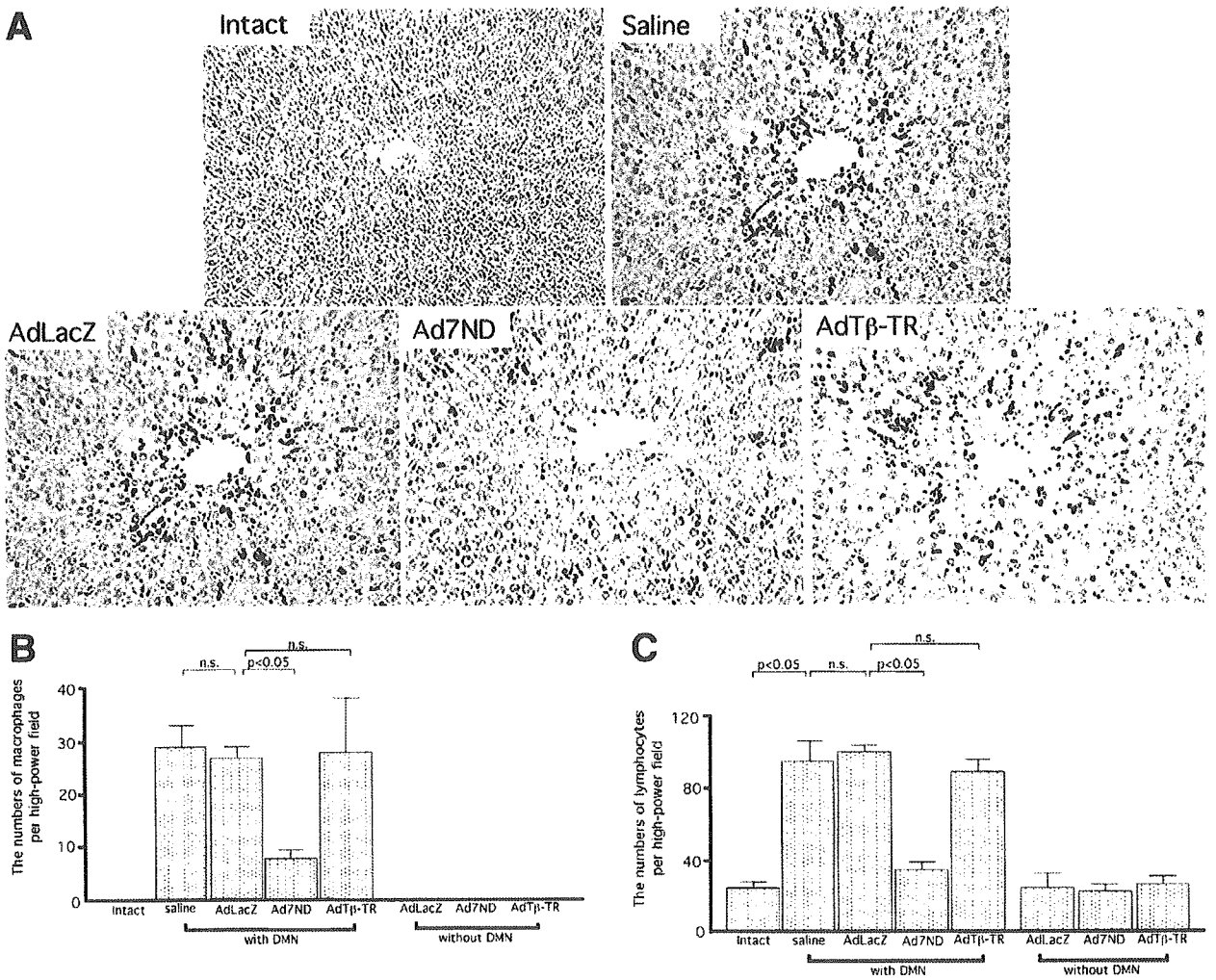


**Figure 3.** Infiltration of macrophages and lymphocytes into DMN-treated livers. Rats were given a single infusion of saline, AdLacZ, Ad7ND, or AdTβ-TR via the tail vein. Seven days later, some rats were administered DMN once (shown as *with DMN*) and some rats were not administered DMN (shown as *without DMN*; histology not shown). Twenty-four hours after the DMN challenge, they were killed, and liver sections were histologically examined either by immunohistostaining against CD68, to detect macrophages (*A*), or by hematoxylin staining for lymphocytes (not shown; original magnification, 200×). Similar histology was seen in all 4 rats in each group. The numbers of (*B*) macrophages and (*C*) lymphocytes were semiquantitated (see Materials and Methods). Four fields in each of 4 rats (a total of 16 fields in each group) were examined, and the number of cells per high-power field is shown as mean ± SD. n.s., statistically not significant. Rats never treated with adenovirus or DMN were also analyzed (shown as *intact*).

β-galactosidase (AdLacZ), a truncated TGF-β receptor (AdTβ-TR), or a mutated MCP-1 (Ad7ND). Seven days later (when the expression of the introduced molecules had reached a submaximal level), DMN was given. One day after a single injection of DMN, we analyzed liver sections by hematoxylin staining and immunohistostaining against CD68, which is a specific marker for macrophages. Macrophages were detectable in the centrilobular area of the livers of AdLacZ-infected, AdTβ-TR–infected, or saline-injected rats: there were no differences among these 3 groups. However, macrophages were greatly reduced in Ad7ND-treated livers (Figure 3*A*). The numbers of CD68-positive cells (per high-power field) were 29 ± 3.5 in saline-treated livers, 27.5 ± 2.1 in AdLacZ-treated livers, 27.5 ± 11.4 in AdTβ-TR–treated livers, and only 7.1 ± 1.2 in Ad7ND-treated livers (Figure 3*B*). Similarly, the numbers of lymphocytes (histology not shown) were 98 ± 7.5 in saline-treated livers, 101 ± 2.5 in AdLacZ-treated livers, 93 ± 5.5 in AdTβ-TR–treated livers, and only 40 ± 3.5 per high-power field in Ad7ND-treated livers (Figure 3*C*). Without DMN treatment, neither macrophages nor lymphocytes (histology not shown) were increased in the livers of AdLacZ-infected, AdTβ-TR–infected, and

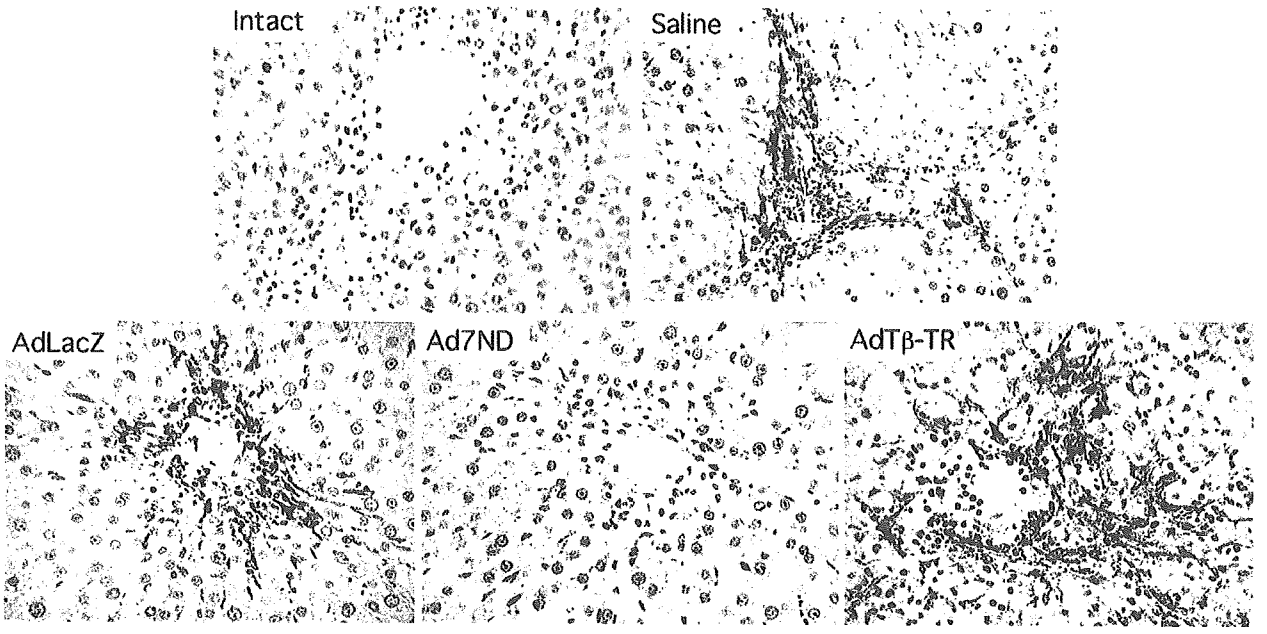


**Figure 4.** α-Actin–positive cells in DMN-treated livers. Rats were treated with either an adenovirus or saline as described in the legend to Figure 3 and then subjected to DMN for 3 consecutive days. One day after the last DMN injection (the fourth day), livers were examined by immunohistostaining against α-actin (original magnification, 200×). Rats never treated with adenovirus or DMN were also analyzed (shown as *intact*). Similar histology was seen in all 4 rats in each group.

Ad7ND-infected livers compared with intact livers (subjected to no injection of either saline or adenovirus and no DMN treatment; Figure 3*B* and *C*).

Next, after a 3-day DMN treatment, we examined livers for α-actin–positive cells (a marker of activated HSC). They were readily detectable, not only in AdLacZ- or saline-treated, but also in AdTβ-TR–treated livers. In contrast, we could see none in the Ad7ND-treated livers (Figure 4).

### Inhibition of Macrophage Infiltration or of Transforming Growth Factor β Signaling Markedly Suppresses Liver Fibrogenesis and Preserves Liver Function

After a 3-week DMN treatment, the hydroxyproline content of livers was measured as a quantitative evaluation of fibrosis (Figure 5). The hydroxyproline contents in the livers of both AdLacZ- and saline-treated rats were approximately 3-fold higher than in intact livers, as previously observed.[10–12] In contrast, in the Ad7ND-treated and AdTβ-TR–treated livers, the hydroxyproline content remained close to the level seen in intact livers.

After the DMN treatment, the serum levels of aspartate aminotransferase, alanine aminotransferase, and total bilirubin were all increased, and both the body and liver weights were decreased, probably because of liver dysfunction. However, these values were preserved or better maintained in the Ad7ND-treated or AdTβ-TR–treated groups (Table 1).

After a 3-week DMN treatment, we analyzed liver histology both by Masson trichrome staining and by immunohistostaining against α-actin. In accordance with the data on hydroxyproline content (Figure 5), both Ad7ND-treated and AdTβ-TR–treated livers showed a fibrotic area that was markedly smaller than that seen in

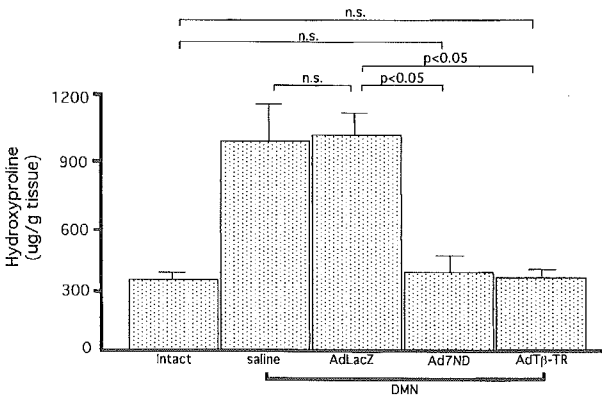


**Figure 5.** Hydroxyproline content of DMN-treated livers. Rats were treated with either adenovirus or saline as described in the legend to Figure 3 and then subjected to a 3-week DMN treatment. Hydroxyproline content of livers is shown as mean ± SD. Three samples from each of 4 rats were analyzed for each group. n.s., statistically not significant. Rats never treated with adenovirus or DMN were also analyzed (shown as *intact*).

**Table 1.** Serum Hepatobiliary Parameters and Body and Liver Weights

| Variable | Total bilirubin (*mg/mL*) | AST (*IU/mL*) | ALT (*IU/mL*) | Body weight (*g*) | Liver weight (*g*) |
|---|---|---|---|---|---|
| Intact | 0.2 ± 0.1 | 68 ± 16 | 40 ± 9 | 350 ± 20 | 3.5 ± 0.1 |
| AdLacZ | 0.2 ± 0.1 | 71 ± 11 | 39 ± 7 | 340 ± 20 | 3.6 ± 0.1 |
| Saline + DMN | 0.7 ± 0.6 | 495 ± 103 | 245 ± 88 | 290 ± 20 | 2.4 ± 0.4 |
| AdLacZ + DMN | 0.8 ± 0.7 | 525 ± 149 | 232 ± 97 | 290 ± 30 | 2.3 ± 0.5 |
| Ad7ND + DMN | 0.3 ± 0.1[a] | 134 ± 16[a] | 69 ± 7[a] | 350 ± 10[a] | 3.4 ± 0.1[a] |
| AdTβ − TR + DMN | 0.4 ± 0.1[a] | 222 ± 84[a] | 69 ± 25[a] | 350 ± 10[a] | 3.5 ± 0.1[a] |

NOTE. Rats were given a single infusion of saline, AdLacZ, Ad7ND, or AdTβ-TR via the tail vein. Seven days later, a 3-week DMN treatment was given to some rats (shown as +DMN). After a 3-week DMN treatment, blood was collected, and body and liver weights were measured. Serum total bilirubin, AST, and ALT and body and liver weights are shown as mean ± SE (n = 4). Rats never subjected to adenovirus infection or treated with DMN were also measured (shown as Intact).
AST, aspartate aminotransferase; ALT, alanine aminotransferase.
[a]$P < .05$ vs. AdLacZ + DMN.

the AdLacZ- and saline-injected rats, and α-actin–positive cells were almost undetectable (Figure 6).

In the AdTβ-TR–treated livers, α-actin–positive cells were readily detectable after the initial 3-day DMN treatment (Figure 4). We assumed that activated HSC disappeared through apoptosis under conditions in which the action of TGF-β was suppressed. We therefore performed TUNEL staining on the fourth day after starting DMN treatment. TUNEL-positive cells were increased in the AdTβ-TR–treated livers; however, no such apoptotic cells were observed in the AdLacZ- or saline-injected livers (Figure 7*A*). Immunohistostaining against α-actin confirmed that the TUNEL-positive cells in the AdTβ-TR–treated livers (Figure 7*A*) were indeed α-actin positive (Figure 7*B*).

## Discussion

Inflammation induces infiltration by leukocytes and monocytes/macrophages into inflamed tissues.[1] Tissue remodeling or fibrosis then follows the inflammation. MCP-1, one of the CC chemokines, attracts monocytes/macrophages bearing CCR2.[1–3] In this study, the roles of such macrophages in injury-induced liver fibrogenesis were investigated by overexpressing a mutated MCP-1 (7ND), which is reported to suppress the actions of MCP-1.[15,23–25] In the Ad7ND-treated rats, DMN-induced infiltration by macrophages and lymphocytes into injured livers was markedly suppressed (Figure 3), the activation of HSC was eliminated (Figure 4), and liver fibrogenesis was greatly prevented (Figures 5 and 6). The cellular infiltration and activation of HSC observed immediately after infliction of the injury were similar between the AdTβ-TR–treated livers and the controls (saline-infused or AdLacZ-infected rats; Figures 3 and 4). Our study shows that infiltrated macrophages are critical for HSC activation and subsequent fibrogenesis and, importantly, that TGF-β is not an activating factor for HSC. It is suggested that the infiltrated macrophages

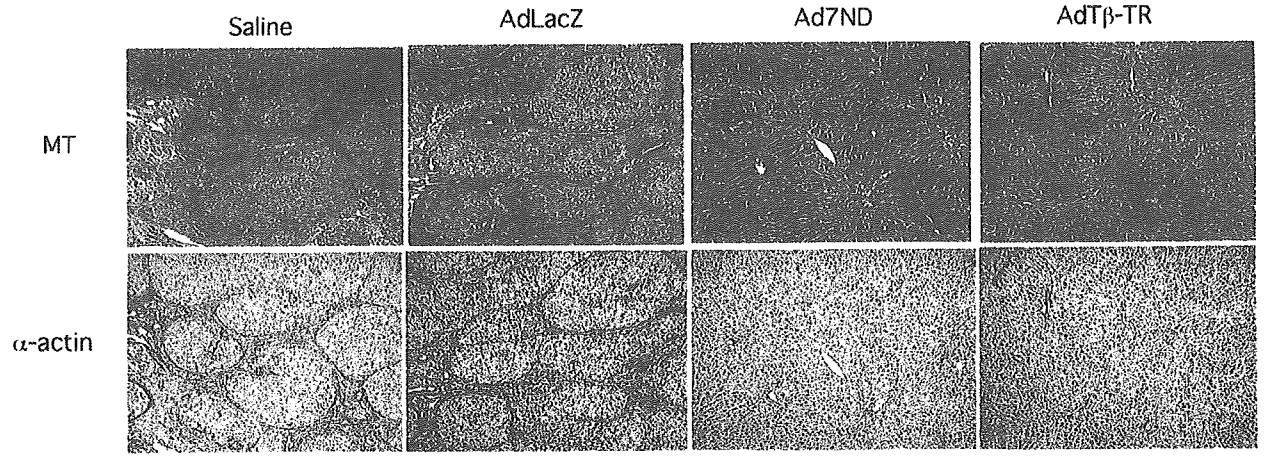


**Figure 6.** Histology of livers after a 3-week DMN treatment. Rats were treated as described in the legend to Figure 5. Liver sections were histologically examined with the aid of Masson trichrome staining (MT) or by immunohistostaining against α-actin (original magnification, 100×). Similar histology was seen in all 4 rats in each group.

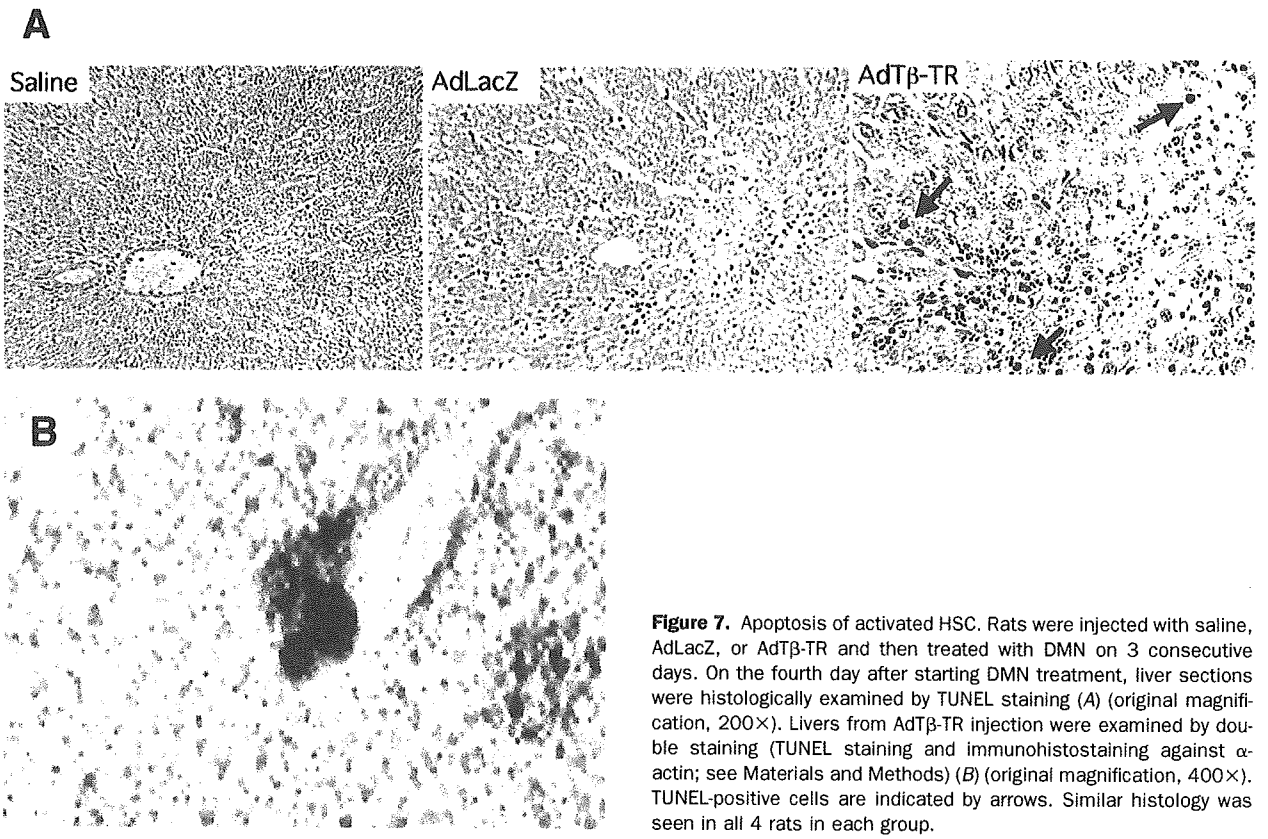


**Figure 7.** Apoptosis of activated HSC. Rats were injected with saline, AdLacZ, or AdTβ-TR and then treated with DMN on 3 consecutive days. On the fourth day after starting DMN treatment, liver sections were histologically examined by TUNEL staining (*A*) (original magnification, 200×). Livers from AdTβ-TR injection were examined by double staining (TUNEL staining and immunohistostaining against α-actin; see Materials and Methods) (*B*) (original magnification, 400×). TUNEL-positive cells are indicated by arrows. Similar histology was seen in all 4 rats in each group.

may themselves secrete an activating factor or factors for HSC.

We have previously shown that anti–TGF-β intervention inhibits liver fibrogenesis[11,13] and its progression.[12] In this study, we found that suppression of infiltration by macrophages and lymphocytes through overexpression of 7ND led to a powerful suppression of liver fibrogenesis to a similar degree as blockade of TGF-β but that the underlying mechanisms seem to be different. Activation of HSC in the initial stage immediately after injury was already eliminated in the Ad7ND-treated livers (Figure 4). Probably because HSC activation was inhibited, the subsequent progress toward fibrosis was suppressed in the Ad7ND-treated livers, thus supporting the idea that activation of HSC is the initial and critical event that leads to liver fibrosis. It has been considered for a long time that TGF-β is the HSC-activating factor (or at least one of the activating factors).[14] However, our study clearly shows for the first time that TGF-β is not the HSC-activating factor, because a substantial number of activated HSC were present in the AdTβ-TR–treated livers (Figure 4); indeed, the numbers of activated HSC were the same among saline-treated, AdLacZ-treated, and AdTβ-TR–treated livers. We confirmed previously that virtually all liver cells are infected with an adenovirus when one is administered to rats with intact livers,[11,13] so the possibility can be excluded that all of these activated HSC were uninfected with AdTβ-TR. Although substantial numbers of activated HSC were seen after a 3-day DMN treatment, most disappeared during the next 2 weeks of DMN treatment (Figure 6). The activated HSC are probably eliminated through apoptosis under conditions in which TGF-β signaling is inhibited. Indeed, we showed that in the AdTβ-TR–treated livers, but not in the AdLacZ- or saline-injected ones, activated HSC were in apoptosis (Figure 7). Saile et al[26] reported that HSC undergo CD95-mediated spontaneous apoptosis when they are activated, and TGF-β inhibits CD95-agonistic antibody-induced apoptosis of activated HSC in culture.[27] On the basis of these reported findings and our present study, it is likely that TGF-β is required for the activated HSC to survive. Consequently, fibrogenesis was markedly inhibited in the AdTβ-TR–treated livers despite activation of HSC in the initial stage after injury. To judge from our findings, anti–TGF-β intervention ought to be superior to anti–MCP-1 therapy for treating liver cirrhosis patients, most of whom already